Dendritic metal complexes for bioimaging. Recent advances

Anne-Marie Caminade, Aurélien Hameau, Cédric-Olivier Turrin, Regis Laurent, Jean Pierre Majoral

Dendritic metal complexes for bioimaging. Recent advances.

Anne-Marie Caminade,[a,b]* Aurélien Hameau,[a,b] Cédric-Olivier Turrin,[a,b] Régis Laurent,[a,b] Jean-Pierre Majoral[a,b]

[a] Laboratoire de Chimie de Coordination, CNRS, 205 route de Narbonne, 31077 Toulouse, Cedex 04, France

[b] LCC-CNRS, Université de Toulouse, CNRS, Toulouse, France

e-mails: anne-marie.caminade@lcc-toulouse.fr; aurelien.hameau@lcc-toulouse.fr; cedric-olivier.turrin@lcc-toulouse.fr; regis.laurent@lcc-toulouse.fr; jean-pierre.majoral@lcc-toulouse.fr

Dedicated to our friend Maurizio Peruzzini on the occasion of his retirement.

Abstract:

Dendrimers are hyperbranched macromolecules, having a large number of terminal functions, easily accessible and modifiable to afford the desired properties. Metal complexes of dendrimers are frequently used as catalysts in diverse reactions, but they can be used also as innovative biological tools. This review focusses on the recent advances (last 10 years) of dendritic metal complexes used for bioimaging, essentially *in vivo*. Three main domains will be covered. The first one concerns luminescent complexes for optical imaging (OI). The second one is the largest one; it concerns magnetic resonance imaging (MRI) contrast agents, mostly based on gadolinium complexes. The third and last domain concerns radioactive dendrimer complexes for single photon emission computed tomography (SPECT), and also for positron emission tomography (PET). Two main radionucleides are used in this context, technetium (^{99m}Tc) and indium (^{111}In). Two types of ligands are generally used for all these complexes in the two last domains, diethylenetriaminepentaacetic acid (DTPA), and a cyclic analogue, 1,4,7,10-tetraazacyclododecane-1,4,7,10-tetraacetic acid (DOTA), and some of their derivatives. These complexes have been used in many cases for *in vivo* imaging of cancerous tumors in mice or rats.

Keywords:

dendrimers; metal complexes; optical imaging; magnetic resonance imaging; single photon emission computed tomography

Abbreviations

ALGD, anionic linear globular dendrimers; AMI, acoustic molecular imaging; APMES, (3-aminopropyl)dimethylethoxysilane; BBB, blood brain barrier; CEST, chemical exchange saturation transfer; CT, computed tomography; β-CD, β-cyclodextrin; Cy5.5, cyanine dye; DGL, dendron-grafted polylysine; DNA, desoxyribonucleic acid; DOTA, 1,4,7,10-tetraazacyclododecane-1,4,7,10-tetraacetic acid; DO3A, 4,7,10-tri(acetic acid)tetraazacyclododecane; DOX, doxorubicin; DTPA, diethylenetriaminepentaacetic acid; EGTA, ethylene glycol tetraacetic acid; EPR effect, enhanced penetration and retention effect; FA, folic acid; Gn, number of generations; GO, graphene oxide; i.v., intravenous; mAb, monoclonal antibody; MAL-PEG3500-NHS, Maleimide-poly(ethyleneglycol)-N-hydrosuccinimide; mPEG, methoxy poly(ethyleneglycol); MR, magnetic resonance; MRI, magnetic resonance imaging; NHS ester, N-hydroxysuccinimidyl ester; NIR, near infra-red; NIRF, near infra-red fluorescence; NO, nitric oxide; NOTA, 1,4,7-triaazacyclononane-1,4,7-triacetate; NP, nanoparticle; OI,

optical imaging; PAI, photoacoustic imaging; PAMAM, Poly(amidoamine); PARACEST, paramagnetic chemical exchange saturation transfer; pEGFP, plasmid of the green fluorescent protein; PEG, poly(ethyleneglycol); PET, positron emission tomography; PPI, poly(propyleneimine); PS, propane sultone; PSCA, prostate stem cell antigen; PSMA, prostate specific membrane antigen; RGD peptide, Arginylglycylaspartic acid peptide; ROS, reactive oxygen species; SAH, succinic anhydride; $SAT(PEG)_4$, N-succinimidyl (S)-acetyl(thiotetraethylene glycol); SCAs, smart or responsive contrast agents; SPECT, single photon emission computed tomography; TIBA, 2,3,5-triiodo benzoic acid; TRAP, triazacyclononane-triphosphinate.

Contents

1. Introduction
2. Luminescent dendrimer complexes for optical imaging
3. Magnetic Resonance Imaging contrast agents based on lanthanide complexes
3.1. Dendritic complexes of Gadolinium for in vivo imaging
3.1.1. DTPA Gd complexes of PAMAM dendrimers
3.1.2. Macrocyclic Gd complexes of PAMAM dendrimers
3.1.3. Macrocyclic Gd complexes of PAMAM dendrimers associated with gold nanoparticles
3.1.4. DTPA Gd complexes of other dendrimers
3.1.5. Macrocyclic Gd complexes of other dendrimers or dendrons
3.2. Dendritic complexes of other metals
4. Radioactive dendrimer complexes for SPECT imaging
4.1. Dendritic complexes of Technetium
4.1.1. Technetium complexes of PAMAM dendrimers
4.1.2. Technetium complexes of other dendrimers
4.2. Dendritic complexes of radioactive ^{111}Indium
4.3. Dendritic complexes of other radioactive elements
5. Radioactive dendrimer complexes for PET imaging
6. Conclusion
7. References

Graphical abstract:

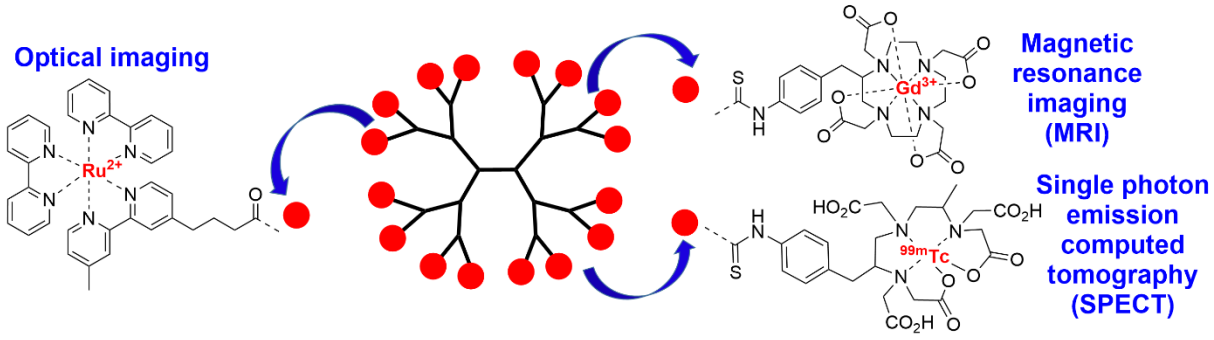

Highlights:

- Dendrimer complexes have many biological properties
- Dendrimer complexes can be specifically engineered for imaging
- Dendrimer complexes can be used for optical imaging
- Dendrimer complexes of gadolinium are useful contrast agents for magnetic resonance imaging *in vivo*
- Dendrimer complexes of ^{99m}Tc or ^{111}In are useful agents for single photon emission computed tomography *in vivo*

1. Introduction

The field of nanomedicine is one of the fastest growing area in research and applications [1], due to its ability to revolutionize diagnostic and therapeutic tools [2], as the nanoscale dimensions play important roles in biological systems. Metal-based (hard) nanoparticles constitute the largest part of nanomaterials used in nanomedicine [3,4] in particular against cancers [5]. However, due to the potential toxicity of hard nanoparticles [6-8], softer alternatives are needed. Dendrimers, especially those complexing metals, appear as an attractive alternative to hard nanoparticles, as they are hyperbranched nanomolecules with defined structures, due to their step-by-step synthesis [9]. The chemical structure of dendrimers can be very different, as illustrated in Figure 1 for the most important types of structures used for bioimaging, namely poly(amidoamine) (PAMAM) [10] and poly(propyleneimine) (PPI) [11,12]. The number of layers gives the number of generations (Gn). However, there is a discrepancy concerning the generation number of commercially available PAMAM dendrimers, and the other dendrimers, as illustrated in Figure 1 with the generations 3 of PAMAM dendrimers, and the generation 4 of PPI dendrimers, both having the same number of terminal functions (32 NH_2 groups).

Most properties of dendrimers depend on the nature of their terminal functions, although recent studies have demonstrated that the inner structure can dramatically influence the way the terminal function are organized and hence affect the biological properties [13]. NH_2 terminal functions of PAMAM and PPI dendrimers are very reactive functions. They afford the possibility to fulfil the desired properties by modifying them, in particular to afford diverse types of biological properties.

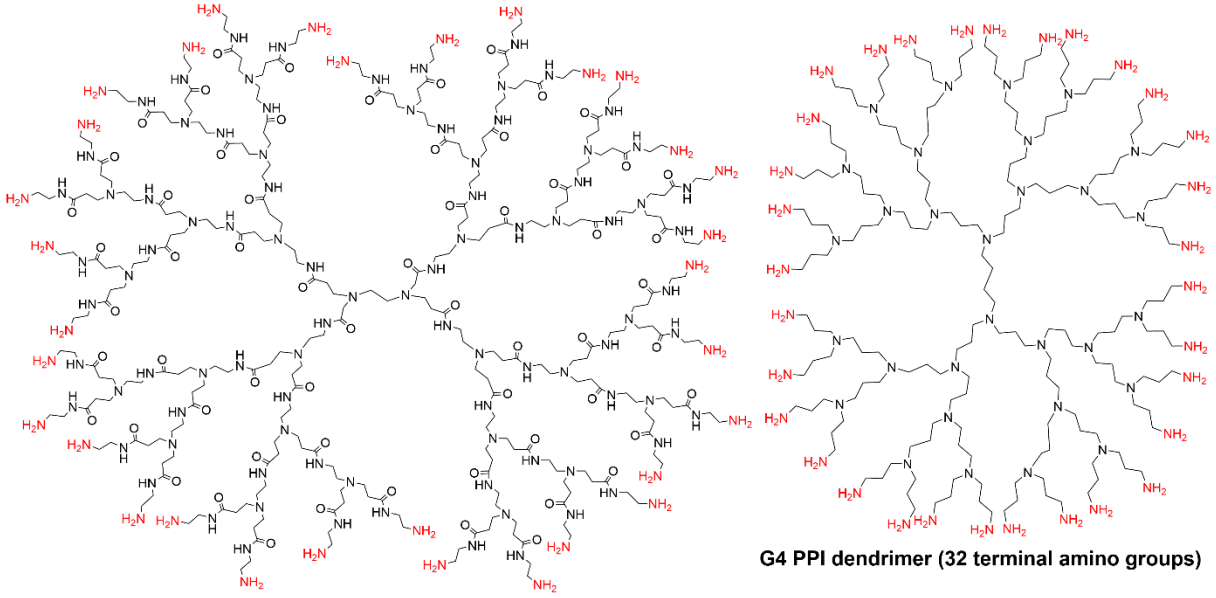

Figure 1. Chemical structure of the third and fourth generations of the two main types of dendrimers used for imaging.

Several advantages are expected to be afforded by dendrimers in biology. Dendrimers are considered as non-immunogenic soft nanoparticles, having size, globular shape, and functionalities comparable to that of many proteins, and have been referred to as “artificial proteins” [14]. Contrarily to hard nanoparticles, dendrimers have a uniform and highly reproducible soft structure, in which size, shape, internal and surface chemistry are highly controlled. The size of dendrimers enables their use for the passive targeting of tumors, thanks to the EPR (enhanced penetration and retention) effect, even if this effect is relatively controversial. Indeed, a long circulation of dendrimers *in vivo* in blood vessels can be expected (if they are not captured by macrophages), as they are less rapidly excreted by kidney compared to small molecules. Furthermore, accumulation in tumors can be observed, due to the presence of abnormal vessels in tumors, having wide fenestrations enabling the penetration of

dendrimers inside the tumor [15]. The presence of a large number of terminal functions easily accessible has two advantages: i) the multiplication of the number of active entities in a single component, to enhance the efficiency, and ii) the possibility to have different functions at the same time, such as one for targeting, while the others afford the desired properties. All these possibilities illustrate the potential role of dendrimers in nanomedicine.

Molecular imaging, i.e. the ability to visualize and quantitatively measure the function of biological and cellular processes *in vivo* has a great impact in medicine. It can be used for detecting diseases at an early stage, identifying the extend of the disease, for selecting therapeutic treatment in personalized medicine, for targeted therapy and for measuring the effects of treatments. The most important techniques of clinical relevance for imaging are mainly positron emission tomography (PET), single photon emission computed tomography (SPECT), magnetic resonance imaging (MRI), optical imaging (OI), and ultra-sounds (US). However other strategies are being explored, such as acoustic molecular imaging (AMI), or photoacoustic imaging (PAI). The potential of all these techniques for clinical molecular imaging has been reviewed [16].

The use of dendrimers for bioimaging, and particularly of dendrimer complexes, is attracting prolific attention, that is the reason why it appears that this field is now worth to be reviewed. The early times have been reviewed in 2012 [17] thus we will concentrate mainly on the work published in the last ten years, since 2011. Despite the large number of references, this review is not fully exhaustive, but it will give a large overview of the usefulness of dendritic metal complexes for bioimaging. Metal nanoparticles entrapped inside dendrimers or covered by dendrimers will not be considered, except if they are associated with discrete complexes of dendrimers. The review will be organized according to the properties of the dendritic complexes. Noninvasive imaging techniques, such as optical imaging (OI), magnetic resonance imaging (MRI), positron emission tomography (PET), single photon emission computed tomography (SPECT), computed tomography (CT), taking advantage of the use of nanomedicine concepts has been reviewed relatively recently [18]. However, this review did not focus on dendrimer complexes. The contribution of dendrimer complexes to these imaging techniques will be reviewed from the chemists' viewpoint, highlighting the type of dendrimers, mainly PAMAM and PPI dendrimers, and the types of ligands, mainly diethylenetriaminepentaacetic acid (DTPA), and a cyclic analogue, 1,4,7,10-tetraazacyclododecane-1,4,7,10-tetraacetic acid (DOTA), and some of their derivatives. The metal complexes are generally located on the surface of dendrimers, but in a few cases, they can be located at the core or within the structure. Emphasis will be put on dendrimers which have been tested for *in vivo* bioimaging, essentially on mice bearing tumors [19].

2. Luminescent dendrimer complexes for optical imaging

Many intrinsically fluorescent dendrimers or dendrimers bearing classical fluorophores in some parts of their structure have been used since a long time for bioimaging [20]. However, very few of such compounds bear metal complexes as the luminescent emitters. They are based on lanthanides, essentially Europium, but also on Ruthenium complexes, most generally located on the surface of the (PAMAM) dendrimers.

An early report concerned the complexation of 8 europium cations within the branches of a generation 3 PAMAM dendrimer functionalized on the surface by 32 naphthalimide fluorophores (Figure 2A). The luminescence emission spectrum of this dendrimer complex indicates the presence of a prominent broad band with a significant component in the red/NIR (near infra-red) part of the electromagnetic spectrum. The eight Eu^{3+} provide an increased stabilization to the electronic structure of the thirty-two 4-amino-1,8-naphthalimide fluorophores. This dendrimer complex was used for detecting hepatic tumors into WAG/RijHsd rats. The dendrimer complex preferentially accumulated within liver tumors *in vivo* and provided a persistent luminescence [21]. The same dendrimer was also used for the detection of multiple metastases into the same type of rats [22].

An esteramide dendrimer was especially engineered and functionalized via different linkers with 8 hexadentate-all-oxygen-donor-ligands suitable for the complexation of lanthanides such as ytterbium, europium, dysprosium, samarium, and gadolinium (Figure 2B), in view of bimodal luminescence in the near infra-red (NIR) and magnetic resonance imaging (MRI). The photoluminescence properties could

be determined only for the Yb derivatives. Some data could be collected by directly exciting Eu in the Eu derivatives, but not for the Sm complexes. Thus, only the Yb derivatives were found suitable for both NIR luminescence and MRI. All these complexes were found non-toxic towards the cancerous HeLa cell line [23].

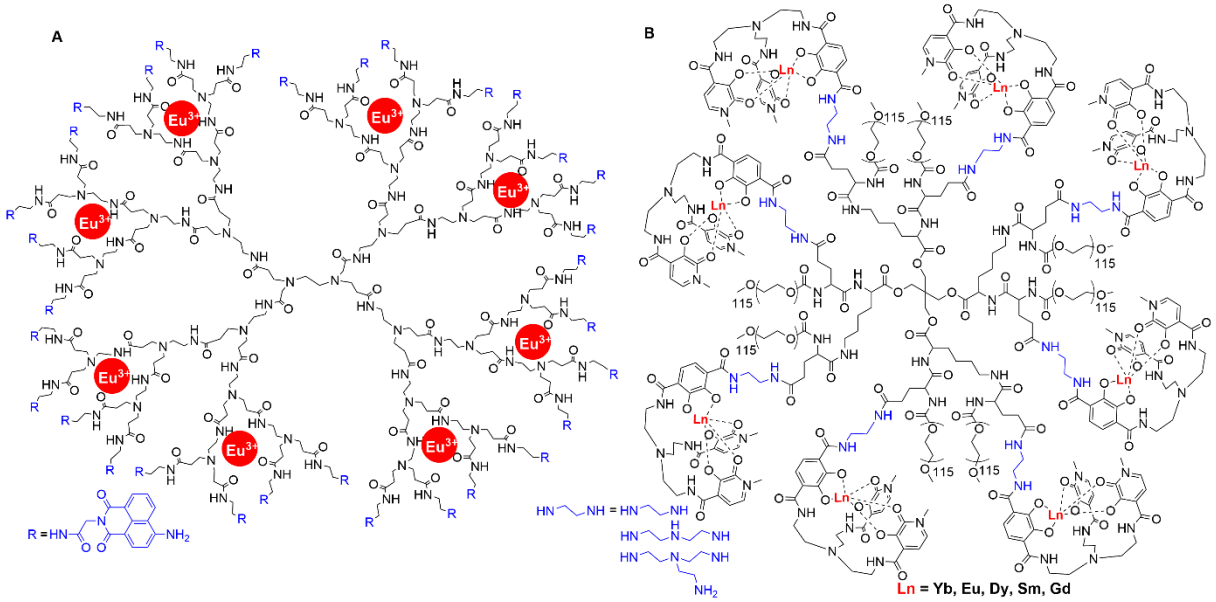

Figure 2. Complexation of lanthanides for luminescence studies.

Beside lanthanides, a few other dendrimers based on tri-pyridyl or tri-bipyridyl iridium or ruthenium complexes were synthesized as fluorescent tools for imaging cells. The properties of small PAMAM dendrimers complexing iridium (Figure 3A) were compared with that of the corresponding monomer. The complexes displayed triplet metal-to-ligand charge-transfer emission. The cellular uptake of the complexes by the human cervix epithelioid carcinoma (HeLa) cell line indicated that all the complexes form very sharp luminescent rings surrounding the cell nuclei. In addition, only the dendritic complexes showed a specific labelling of the Golgi apparatus [24].

PAMAM dendrimers with cystamine core and sixteen surface amino groups were decorated with a bipyridine or phenanthroline derivative, and used for the complexation of ruthenium, as shown in Figure 3B. Both complexes are brightly fluorescent. Fluorescence microscopy images of these dendrimers incubated with CT26 colon carcinoma cells indicate that both dendrimers accumulated first in the cells through retention in the lipid membranes. These nanosized dyes were then internalized via passive endocytosis, and accumulated in the lysosome. Both dendrimers produced comparable amounts of singlet oxygen upon irradiation [25].

An hexanuclear ruthenium(II) polypyridyl complex (Figure 3C) could stepwise condense DNA *in vitro* and possesses outstanding photochemical properties. This compound was used to track the delivery of the plasmid pEGFP (green fluorescent protein) DNA into HeLa cells, using one- and two-photon imaging. With two-photon microscopy, a high signal-to-noise contrast was achieved by irradiation with an 830 nm laser. Merged fluorescence images between Hoechst 33258 (blue staining of the nuclei) and the Ru complex condensing pEGFP DNA demonstrated that the transfection occurred, as shown by the detection of the expression of EGFP after 12h (Figure 3D) [26].

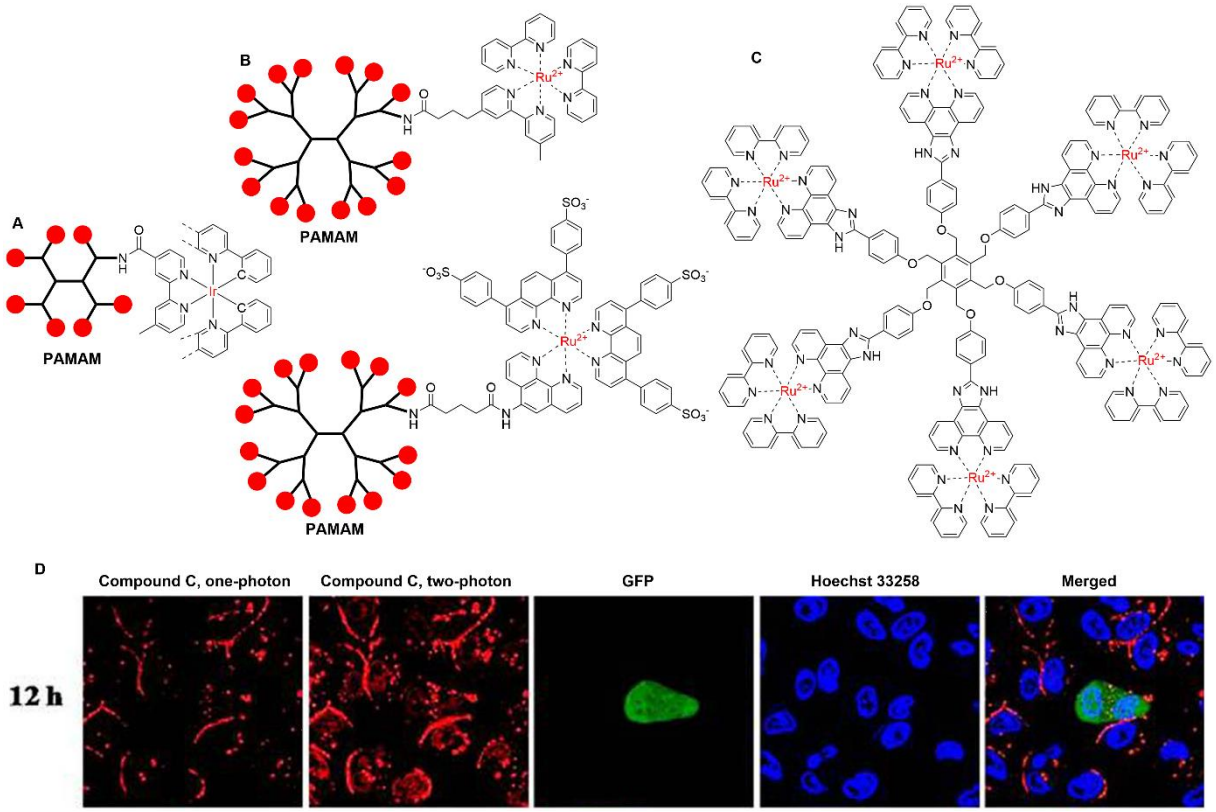

Figure 3. Luminescent dendrimers based on tri-pyridyl or tri-bipyridyl complexes of iridium and ruthenium. Part (D): confocal microscopy images of entry and transportation in Hela cells of the Ru complex shown in C condensing pEGFP DNA (reproduced from ref. 26. Copyright H. Chao et al., open access article).

3. Magnetic Resonance Imaging contrast agents based on lanthanide complexes

Magnetic resonance imaging (MRI) is a powerful non-invasive imaging technique that does not use ionizing radiation. MRI can detect diseases, and can also help in monitoring disease progression and treatment. MRI images are produced by mapping either the relaxation rates or densities of the nuclear spins of water protons in a magnetic field. The relaxation rates are due in part to the chemical composition of the environment. However, the differences in the signal intensities are generally not sufficient to produce a satisfactory contrast. Therefore, contrast agents able to catalytically accelerate the relaxation rate of water, providing contrast-enhanced images, are of great importance. Paramagnetic compounds based essentially on gadolinium, but also on manganese complexes, influence the longitudinal relaxation rate (T_1), whereas superparamagnetic iron oxide nanoparticles influence the transverse relaxation rates (T_2) [27]. Different MRI contrast agents are on the market since more than fifteen years, mainly based on gadolinium complexes, such as Magnevist®, or Dotarem® [28].

The use of dendrimers as contrast agents for MRI has been recognized very early, using PAMAM dendrimers functionalized with gadolinium complexes of diethylenetriaminepentaacetic acid (DTPA) [29], or 4,7,10-tri(acetic acid)tetraazacyclododecane (DO3A) [30]. The early time of macromolecular imaging agents, including dendrimers, has been reviewed in 2012 [31]. Several reviews specialized on dendrimers used as magnetic contrast agents have been proposed more recently [32,33]. In the paragraphs below, we will focus on dendritic complexes of gadolinium and other lanthanides, used as magnetic contrast agents for *in vivo* imaging, since 2011.

3.1. Dendritic complexes of Gadolinium for in vivo imaging

This section is organized depending on the type of dendrimers (PAMAM or other dendrimers), and also on the type of ligands, either branched ligands, or macrocyclic ligands.

3.1.1. DTPA Gd complexes of PAMAM dendrimers

Diethylenetriaminepentaacetic acid (DTPA) has a high affinity for metal cations, as a potential octadentate ligand (5 CO_2H, 3 N). DTPA is used as the ligand for gadolinium in the first intravenous contrast agent to become available for clinical use in 1987 under the name of Magnevist®, which is in widespread use around the world. The grafting of DTPA to dendrimers was carried out with the aim of enhancing the relaxivity properties, and thus the contrast of MR images, due to the presence of a large quantity of paramagnetic ions. The grafting to dendrimers necessitates the presence of an additional function on DTPA, frequently an isothiocyanatobenzyl function, suitable for reacting with the NH_2 terminal functions of PAMAM dendrimers. In the very first example (Figure 4A), all the terminal functions of second generation PAMAM dendrimer were functionalized [29]. Later on, larger dendrimers were used. For instance, a generation 6 PAMAM dendrimer was functionalized with DTPA, then used for complexing 204 Gd^{III} ions. This dendrimer was applied as MRI contrast agent for the lymphatic system in mice [34].

In other cases, only a limited number of terminal functions were of type DTPA for the complexation of gadolinium, together with other functions. This stochastic functionalization provides a mixture of dendrimers equipped with a different number of functions. For instance, a generation 4 PAMAM dendrimer (64 NH_2 surface groups) was first functionalized with biotin (9.9±1.3 or 1.0±0.1) and then by DTPA complexing Gd (43.6±1.9 or 47.6±2.2), the remaining functions being unreacted NH_2 (Figure 4B). These dendrimers were used *in vivo* for imaging mice bearing FM3A (mouse breast carcinoma) tumors [35]. PAMAM generation 5 dendrimer (128 NH_2 surface groups) was first reacted with 10 equivalents of MAL-PEG3500-NHS (Maleimide-polyethyleneglycol-N-hydrosuccinimide). Reaction occurred exclusively on the NHS side of the PEG. Then 87 DTPA derivatives were grafted, and used for the complexation of gadolinium, affording again a stochastically functionalized dendrimer. Five min after the injection of the dendrimer in mice with subcutaneous Bel-7402 xenografts (human liver cancer), tumor appeared hyper intense in the MRI images [36].

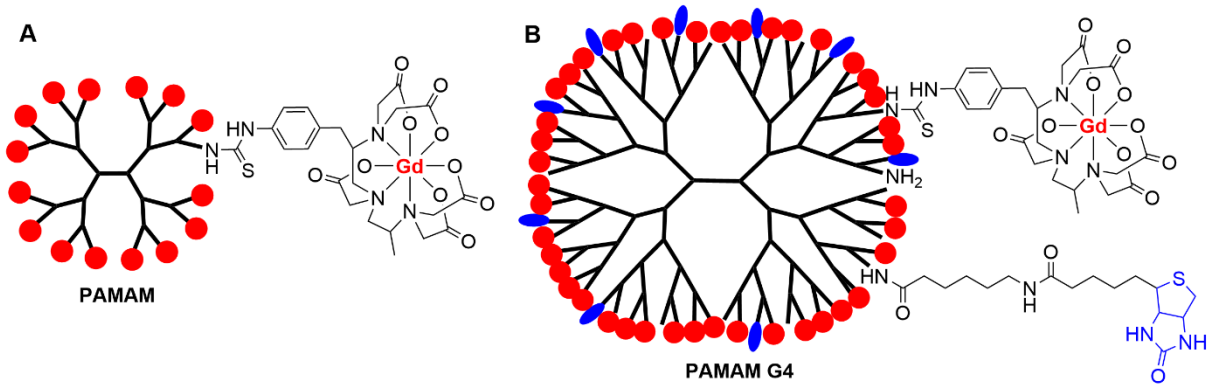

Figure 4. PAMAM dendrimers functionalized with DTPA complexing Gd^{III}; only one of the possible isomers is shown in case B.

PAMAM dendrimers functionalized with DTPA were also associated with diverse nanomaterials. LAPONITE® nanodisks with a diameter of 25 nm and 1 nm thickness are synthetic clay materials. They have been sequentially functionalized with (3-aminopropyl)dimethylethoxysilane (APMES), then with succininc anhydride (SAH) to provide carboxylic acids. Then, the second generation PAMAM dendrimer was reacted, and subsequently modified with DTPA, then with gadolinium, as shown in Figure 5A. These functionalized nanodisks did not display cytotoxicity in the concentration range 0-200 µg/mL. They were injected to BALB/c nude mice bearing a xenografted tumor of HeLa cells. The subcutaneous tumor appeared brighter than the adjacent tissues, showing that the nanodisks functionalized by the dendrimers complexing gadolinium efficiently penetrated inside the tumor [37]. In a recent example, graphene oxide (GO) nanosheets were functionalized by gadolinium-labeled PAMAM nanoclusters. The first step was the formation of the nanoclusters by reacting PAMAM dendrimers generation 5 with HOOC-PEG-COOH. The cluster was then reacted with DTPA dianhydride, and finally with gadolinium

ions, affording GdDN. On the other hand, graphene oxide was prepared from the reaction of graphite power with concentrated HNO_3, then with $KMnO_4$, and finally with H_2O_2. In the last step, the nanocluster was reacted with GO (Figure 5B). HepG2 cells incubated with different concentrations of GO-GdDN displayed no significant decrease in viability, indicating a good biocompatibility. The pharmacokinetic studies in nude mice indicated a longer retention time, compared to the dendrimer alone or to the nanocluster. It was shown that GO-GdDN essentially accumulated into the kidney. However, a few minutes (15 to 90) after injection, a rapid accumulation in the liver was observed by MRI, indicating that GO-GdDN could be a potential candidate to accurately diagnose liver lesions [38]. A PAMAM dendrimer built from a benzene core was also used for the functionalization of graphene oxide; a large part of the remaining NH_2 groups were functionalized by DTPA used for complexing Gd. One or a few NH_2 groups were used for the grafting of prostate stem cell antigen (PSCA) monoclonal antibody (mAb). The *in vivo* magnetic resonance imaging results indicate that this functionalized dendrimer linked to GO can be used as a targeted contrast agent for prostate tumor imaging. Furthermore, loading of doxorubicin hydrochloride (DOX) allowed to demonstrate the targeted delivery to malignant prostate tumors and the inhibition of tumor growth in nude mice (Figure 5C) [39].

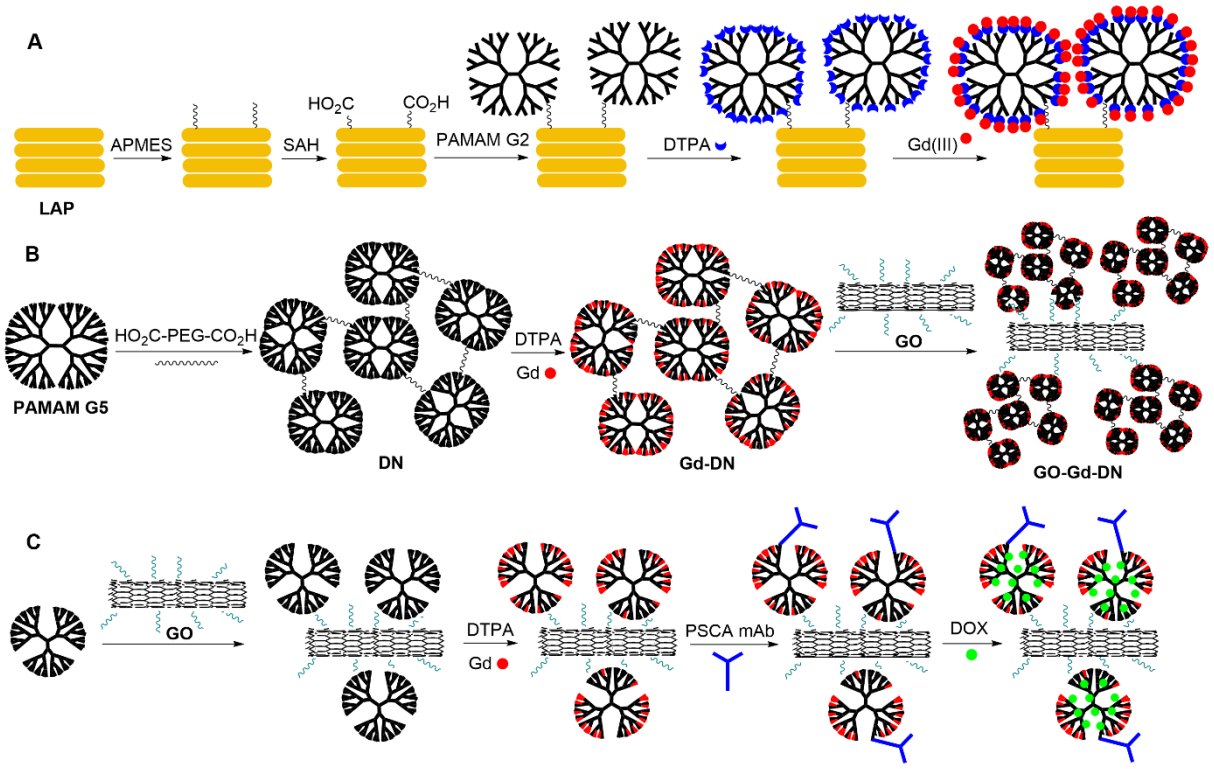

Figure 5. PAMAM dendrimers functionalized with DTPA-Gd complexes, and associated with Laponite (A) and graphene oxide (B and C).

3.1.2. Macrocyclic Gd complexes of PAMAM dendrimers

The macrocycle-structured gadolinium-based MRI contrast agent Dotarem® is the trade name of Gadoteric acid, based on the complexation of gadolinium with the macrocyclic 1,4,7,10-tetraazacyclododecane-1,4,7,10-tetraacetic acid (DOTA). The introduction of a macrocyclic tetraazapolyacetate ligand instead of DTPA should improve the kinetic inertness and thermodynamic stability of the Gd complexes. Grafting DOTA to the surface of dendrimers necessitates the presence of an additional function, which can be linked to one carbon of the macrocycle, preserving the 4 carboxylic acids of DOTA, or linked to one nitrogen of the macrocycle, thus preserving only 3 carboxylic acid function, and affording the so-called DO3A macrocycle (note that DO3A macrocycles are also frequently named DOTA). In most cases, the additional function is an isothiocyanate, suitable for reacting with the NH_2 terminal functions of PAMAM dendrimers. The first example of a macrocycle

complexing gadolinium on the surface of PAMAM dendrimers was of type DO3A. The number of complexes per dendrimer depended on the generation, but not all terminal NH_2 group could be functionalized. 23 Gd were complexed by generation 3 (instead of 32), 30 by generation 4 (instead of 64) and 52 by generation 5 (instead of 128) (Figure 6A) [30]. Later on, DOTA was grafted to generations 4 (28 Gd), 5 (61 Gd), and 6 (115 Gd) (Figure 6B), and used for imaging female nude mice [40].

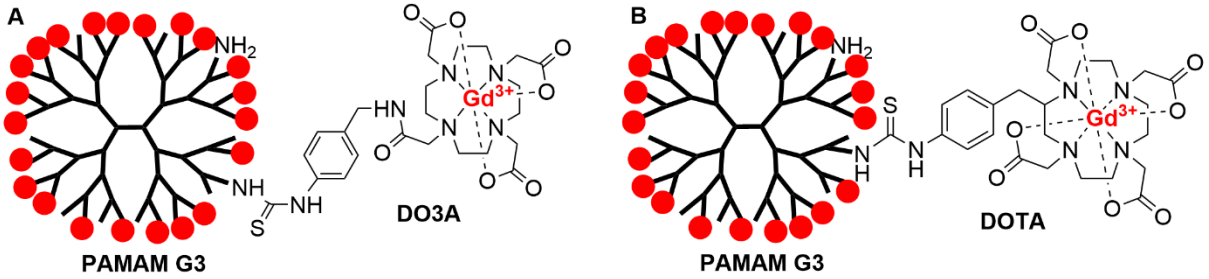

Figure 6. DO3A and DOTA macrocycles complexing gadolinium.

As already indicated for PAMAM dendrimers bearing DTPA complexes, in most cases other functional groups than DOTA complexes are added on the surface of dendrimers. For instance, dendrimer nanoclusters, analogous to those shown in Figure 5 but using a different linker, have been obtained. PAMAM G3 dendrimer was first reacted with N-succinimidyl (S)-acetyl(thiotetraethylene glycol ($SAT(PEG)_4$). Approximately 13 protected thiol groups were incorporated onto each dendrimer. The polydisulfide cross-linked nanoclusters were obtained by deprotecting the thiol groups on the thiolated dendrimers with NH_2OH,HCl. The association of the thiol groups forming disulfide bridges was stopped when the desired size of dendrimer nanoclusters was reached (59, 91 and 142 nm), by quenching the remaining thiol groups with maleimide. Finally, these nanoclusters were subsequently functionalized with the isothiocyanate of the DOTA-Gd complex (Figure 7A). These clusters were administered intravenously into nu/nu mice. A significant contrast enhancement in the MR images was clearly visible in the kidneys and abdominal aorta [41].

However, in most cases the stochastic functionalization of PAMAM dendrimers was carried out onto isolated molecules, not clusters, as shown in Figure 7A. Multimodal optical/paramagnetic nanoprobes based on generation 5 PAMAM dendrimers were elaborated with the aim of crossing the blood brain barrier (BBB), for brain tumor imaging by a dual mode. For instance, the dendrimer was functionalized with a NIR dye, DyLight680 (DL680), and DOTA complexing Gd. 54 DOTA-Gd and 1.1 DL680 dye were grafted per G5 dendrimer, affording G5-DL680 (Figure 7B). This compound was used as dual probe imaging for a rat with a U-251 glioma. Both NIR fluorescence and MR imaging displayed the accumulation of this dendrimer inside the tumor (Figure 7C) [42]. The same dendrimer was used for targeting triple negative breast cancer. In that case also, it was demonstrated by dual imaging in a subcutaneous flank tumor mouse model of MDA-MB-231 TNBC that the dendrimers G5-DL680 accumulated into tumor selectively (Figure 7D) [43].

Other types of dual probes were obtained by the sequential functionalization of PAMAM generation 5 dendrimer with N-hydroxysuccinimidyl (NHS) esters of rhodamine, Cy5.5 and PEG2000, then with DOTA-NHS, and Gd^{3+}, to afford G5-PEG. The use of the bifunctional 3-(2-pyridyldithio) propionate–PEG2000–maleimide instead of the NHS ester of PEG2000, followed first by the same sequence of reactions than previously, then by the reaction of the angiopep-2 peptide on the pyridyldithio propionate afforded G5-Angio. It was shown that 5 peptides and 50 DOTA-Gd complexes were stochastically grafter per G5 dendrimer. This peptide was shown to cross the BBB. Both dendrimers were used for MR and NIR fluorescence imaging of an orthotopic U87MG glioblastoma tumor in a mouse head. Only G5-Angio was able to cross the BBB, and to delineate the tumor margin [44]. Analogous dendrimers, bearing in addition the tumor vasculature targeted cyclic [RGDyK] peptides were also synthesized, affording G5-RGD and G5-RGD-Angio (Figure 7B). Both dendrimers were used as well for imaging U87MG glioblastoma tumor in mice. Biodistribution studies showed that G5-RGD-Angio has the highest concentration of the four different dendrimers in the brain and in the brain tumor, allowing the best detection by MRI and NIR fluorescence [45].

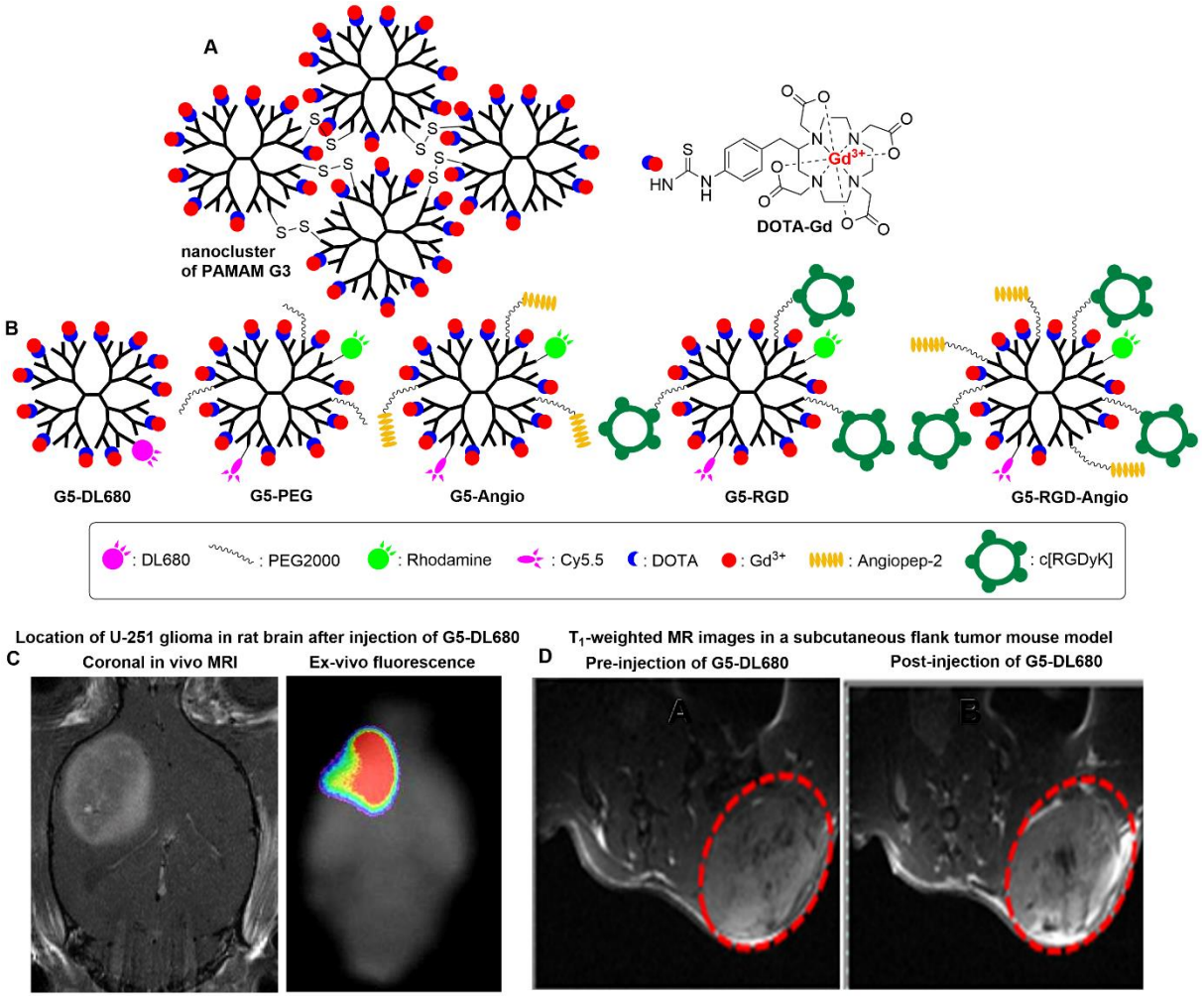

Figure 7. Schematized nanocluster and dual probe imaging dendrimers for NIR fluorescence and MRI, built on generation 3 or 5 PAMAM dendrimers, bearing several DOTA-Gd complexes on the surface. Only one of the possible isomers is shown in all cases (A and B). Part (C): *in vivo* MRI and ex-vivo fluorescence of brain tumor after injection of G5-DL680 shown in part (B)(reproduced from ref. 42. Copyright K. Karki et al., open access article). Part (D): *in vivo* MRI of a subcutaneous flank breast cancer tumor in mouse before and after injection of G5-DL680 (reproduced from ref. 43. Copyright L. Zhang et al., open access article).

The presence of both DO3A Gd complexes and folic acid as a targeting peptide was obtained via non-covalent interactions between PAMAM dendrimers of generation 2.5 (32 carboxylic acid terminal groups) functionalized by β-cyclodextrin (β-CD), and adamantane, as shown in Figure 8. A polyglycerol was functionalized on one side by adamantane, and on the other side by folic acid (Figure 8A), for targeting tumor tissue. Another polyglycerol was functionalized on one side with adamantane, and with pendant chains bearing DOA3-Gd chelates on each end (Figure 8B). Both types of compounds were reacted with a PAMAM dendrimer functionalized with β-CD. This host-guest compound was successfully used for imaging xenograft KB tumor-bearing female athymic nude mice [46].

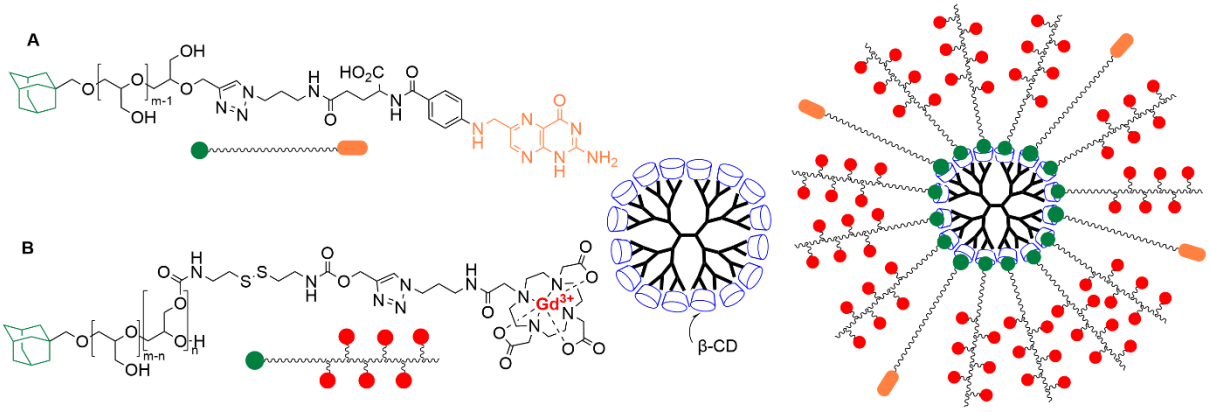

Figure 8. Host-guest interactions for the non-covalent functionalization of PAMAM dendrimers with adamantyl derivatives bearing DO3A ligands complexing Gd.

Smart or responsive contrast agents (SCAs) are molecular sensors capable of altering their magnetic properties upon changing their local environment. Such property enables the assessment of biological processes *in vivo* at the cellular and molecular levels. A series of PAMAM dendrimers were functionalized with a long linker incorporating an ethylene glycol tetraacetic acid (EGTA)-derived Ca-chelator, and various bridges towards the DO3A-Gd complex (Figure 9). These dendrimers were synthesized to follow the dynamics of Ca^{2+} transients or neurotransmitter release. The first example concerned a first generation (8 terminal functions) and a $(CH_2)_3$ linker. This compound was used for *in vivo* MRI after administration into a rat cerebral cortex, showing a robust signal increase [47]. The synthesis was then extended to generation 0 (4 functions), and 2 (16 functions) [48]. A series of generation 4 dendrimers (64 NH_2 groups) possessing the different linkers shown in Figure 9 was also synthesized. An average loading of 52 to 77% in DOTA was observed with all dendrimers [49].

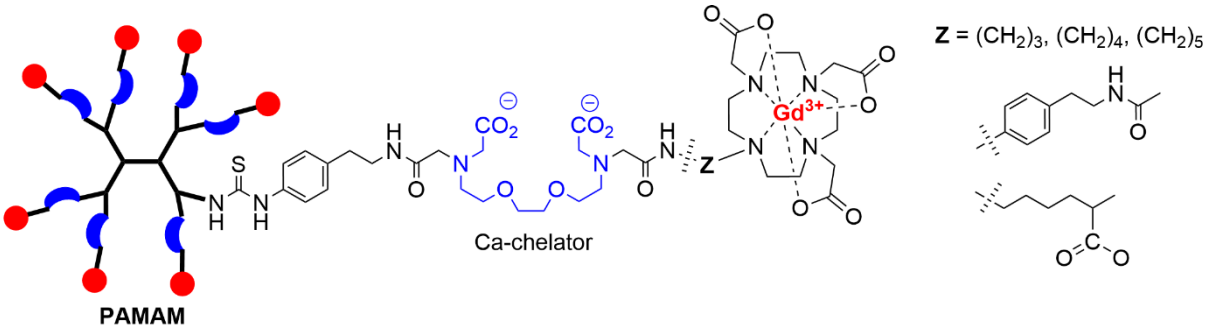

Figure 9. Dendrimers functionalized with both Ca-chelators and DO3A (or DOTA) Gd-complexes.

3.1.3. Macrocyclic Gd complexes of PAMAM dendrimers associated with gold nanoparticles

Many examples of gold nanoparticles entrapped inside PAMAM dendrimers are known, but are out of the scope of this review, as already indicated. However, in some cases PAMAM dendrimers functionalized with DOTA complexing gadolinium and entrapping gold nanoparticles (NPs) have been used for dual imaging, and will be displayed in this paragraph. This association affords the possibility to perform MR imaging thanks to gadolinium, and computed tomography (CT), which is based on many X-ray measurements taken from different angles, thanks to the gold NPs used as contrast agents. As already illustrated in Figure 7, many different functions can be linked stochastically to the surface of a PAMAM dendrimer. The sequential modification of generation 5 PAMAM dendrimers has been carried out with DOTA-NHS and mPEG-COOH. Then, the reduction of $HAuCl_4$ with $NaBH_4$ produced gold NPs entrapped in the dendrimers. Gadolinium was then added to be complexed by DOTA, and finally the remaining NH_2 functions were modified with acetic anhydride, to afford dendrimer G5-Gd-PEG-Au (Figure 10). This nano-assembly was used for CT/MR dual mode imaging of the heart, liver, kidney, and bladder of rat or mouse. *In vivo* biodistribution studies revealed that the G5-Gd-PEG-Au has an extended blood circulation time and can be cleared from the major organs within 24 h [50]. The same

compound was used for dual imaging of xenograft MCF-7 tumor (breast cancer) in male 4-week-old BALB/c nude mice [51]. Replacing mPEG with PEG functionalized with the hypoxia-responsive moiety 2-nitroimidazole afforded the dendrimer G5-Gd-PEGNO_2-Au, suitable for imaging and sensitized radiation therapy of hypoxic tumors (Figure 10). This dendrimer is able to produce reactive oxygen species under X-ray irradiation, promoting DNA damages and preventing DNA repair, and thus affording an efficient dual mode CT:MR imaging of tumor hypoxia, as tested in mice [52].
The same sequence of reactions was carried out using in addition a PEG functionalized with folic acid for targeting tumors (PEG-FA), affording dendrimer G5-Gd-PEG-FA-Au (Figure 10). This nanoprobe was used for dual imaging CT/MRI of a xenograft KB tumor model in male BALB/c nude mice, enabling an effective enhanced tumor contrast. *In vivo* biodistribution indicated that the level of Au in all the major organs at 96h post injection was almost similar to that before injection, suggesting that the nanoprobe is able to be cleared out rapidly from the body [53]. An analogous synthetic process used a PEG functionalized with the RGD peptide (arginine-glycine-aspartic acid), which has been identified as a promising targeting ligand for cancer cells overexpressing $\alpha_v\beta_3$ integrin (Figure 10). Dual mode imaging was carried out successfully with the same type of mice bearing a xenografted U87MG tumor model (human glioblastoma) [54]. Using 1,3-propane sultone (1,3-PS) instead of mPEG in the dendrimer functionalized with DOTA-Gd and the RGD peptide, and entrapping gold NPs afforded a dendrimer bearing zwitterions on the surface, due to the opening of 1,3-PS (Figure 10). This compound was used for dual mode imaging of B16 lung cancer metastasis in mice [55].
An extension of this work concerned the synthesis of a PAMAM dendrimer suitable for trimodal imaging by X-ray computed tomography, magnetic resonance, and optical imaging (CT/MRI/OI). In addition to DOTA, PEG-FA for targeting, and mPEG, the dye Cy5.5 was grafted, before the reduction of $HAuCl_4$ by $NaBH_4$, and finally the complexation of gadolinium, affording compound G5-Gd-PEG-FA-Cy5.5-Au (Figure 10). This compound was used for targeting and for trimodal imaging of xenograft NCI-H460 tumors (human non-small cell lung cancer cells) in BALB/c nude mice [56].

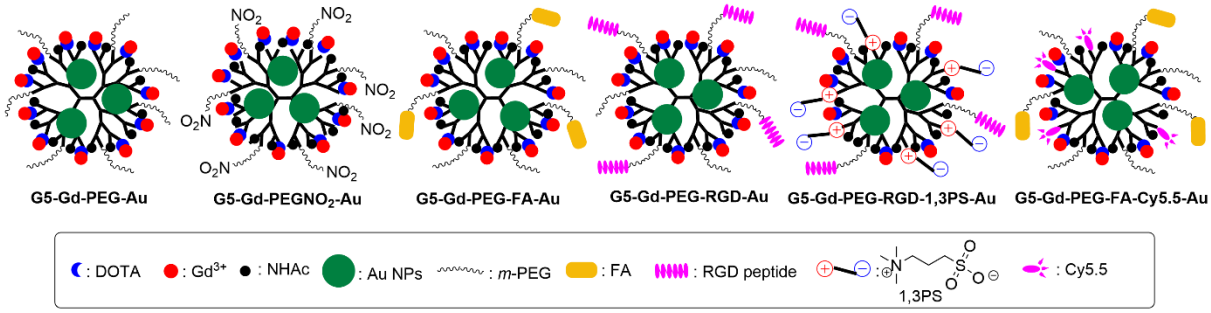

Figure 10. Schematized generation 5 PAMAM dendrimers functionalized with DOTA-Gd complexes and entrapping gold nanoparticles for dual (MRI and CT) or trimodal (MRI, CT and fluorescence) imaging. Only one of the possible isomers is shown in all cases.

3.1.4. DTPA Gd complexes of other dendrimers

Contrarily to PAMAM dendrimers, in which DOTA complexes of gadolinium are the most widely used, DTPA and DOTA complexes of other types of dendrimers are almost equally used. Several polypeptides dendrimers and dendrons (dendritic wedges), most generally based on lysine, have been functionalized with DTPA complexes of gadolinium. An L-Lysine dendron having a carboxylic acid at the core and decorated on the surface by galactosyl moieties was functionalized inside the structure by DTPA complexes of gadolinium. The largest compound incorporated precisely 8 gadolinium complexes linked inside its structure (Figure 11 A). The nanoprobe provided good signal intensity enhancement in mouse liver [57]. Dendrimers based on lysine branches incorporating 12 Gd complexes in the structure and functionalized on the surface by either carboxylic acid or mPEG2000 have been also synthesized (Figure 11 B). The PEGylated dendrimer was used *in vivo* for MR imaging of mouse liver and kidney [58]. Dendron-grafted polylysine of generation 3 (DGL, an hyperbranched polymer of lysine, synthesized in 3 steps) was used as support of a pancreatic tumor-targeting peptide U11, DTPA-Gd complex for MRI, and a near-infrared fluorescent cyanine dye Cy5.5 for optical imaging (Figure 11 C).

This compound was used for ultra-early detection of pancreatic pre-cancerosis in SD rats [59]. This work is related to a previous work using DGL G3, also decorated with DTPA-Gd, and PEG3500, functionalized or not with a choline derivative that affords BBB (blood brain barrier) permeability (Figure 11D). These compounds, as well as monomeric DTPA-Gd, were used for dynamic MRI in glioma-bearing nude mice. The greatest contrast enhancement with the monomeric DTPA-Gd was observed 5 min. after i.v. (intravenous) injection, and then decreased rapidly. The dendritic compound DGL-Gd-PEG produced a slight contrast enhancement during the first 2 hours, and then plateaued for 24h. A significant increase in the contrast enhancement for 24h was observed with DGL-Gd-choline, confirming an increased penetration through the BBB. The images obtained with this DGL clearly delineated the tumor boundary (Figure 11E) [60].

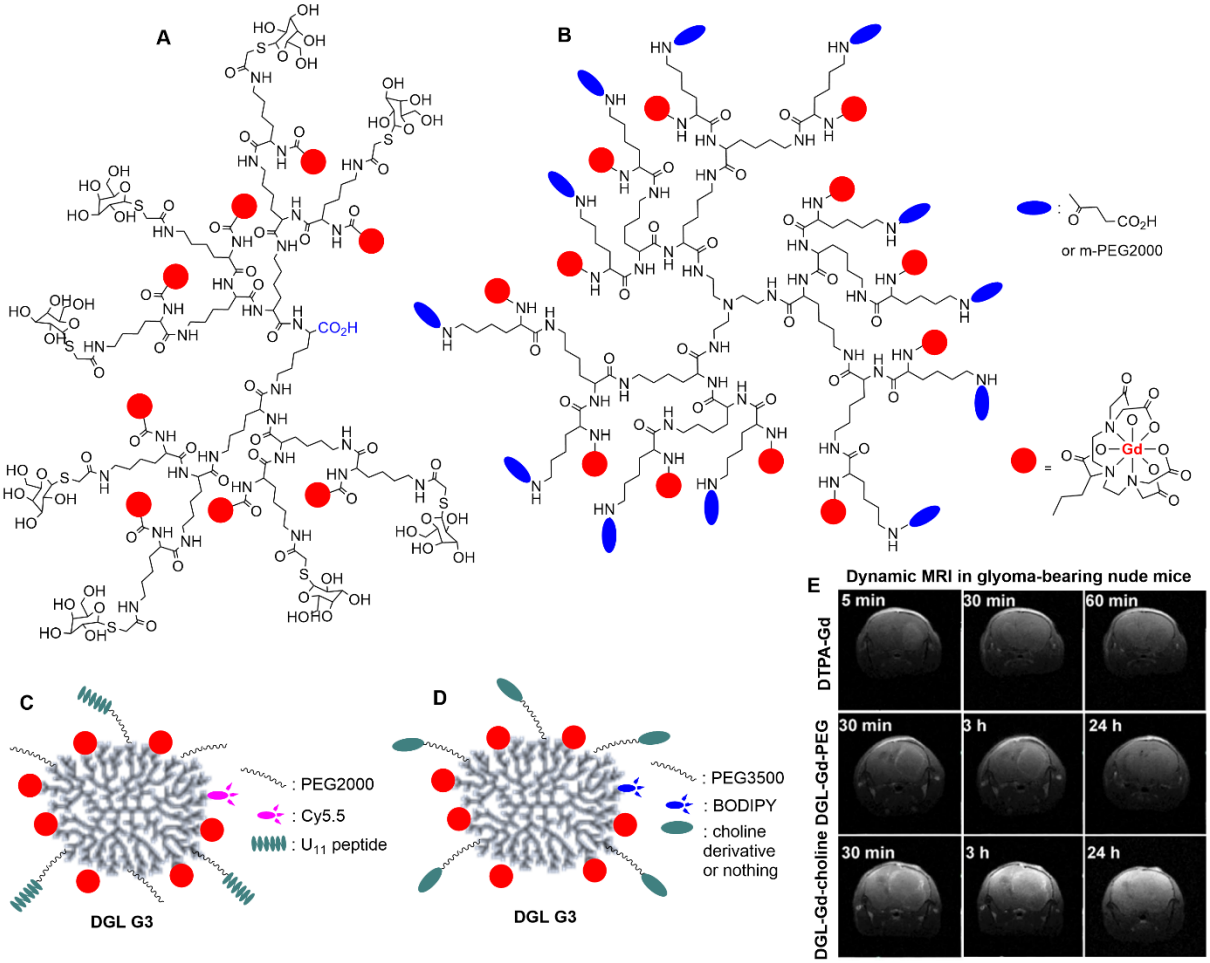

Figure 11. Dendron (A) dendrimer (B) based on L-lysine units, and bearing DTPA-Gd complexes inside their structure. Dendrigraft polylysine (C and D) bearing a few gadolinium complexes on the surface; only one isomer is shown in these cases. Images in (E) are dynamic MR images of the brain in glioma-bearing nude mice obtained with monomeric DTPA-GD, and DGL-Gd functionalized with PEG or PEG equipped with a choline derivative (reproduced from ref. 60. Copyright C. Jiang et al., open access article).

Two generations (3 and 5) of dendrimers based on 1,3,5-triazine as branching points were synthesized and functionalized on the surface by DTPA complexes of gadolinium, as shown in Figure 12 for the third generation. The well-known sequential functionalization of triazine permitted to introduce also alcohol groups on the surface. *In vivo* experiments carried out with mice showed that the third generation was rapidly excreted from the urine, contrarily to the fifth generation [61].

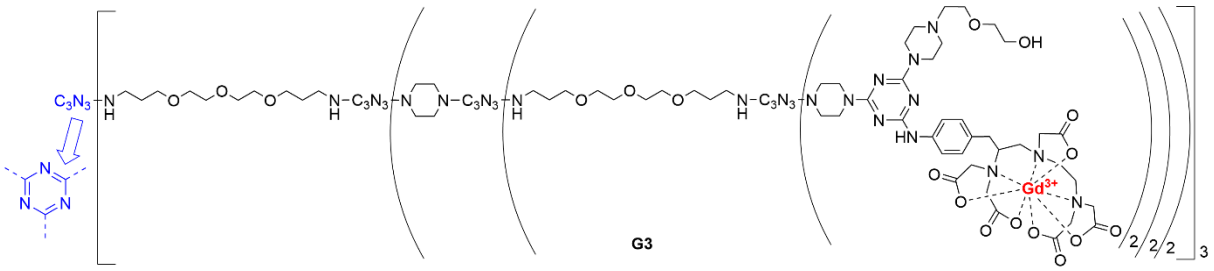

Figure 12. A third generation triazine dendrimer functionalized by both alcohol and DTPA-Gd complex

Another series of compounds are based on biodegradable polyester scaffolds, for a rapid clearance from the body, with limited metabolization inside the cells, which induces the release of toxic Gd^{3+} ions. Several examples are based on β-cyclodextrin core possessing 21 hydroxyl groups, all of them being used for the growing of dendritic branches obtained by the sequential reaction of 2-hydroxyethylmethacrylate and cysteamine. The nitrogen atoms at the branching points of the structure can be functionalized or not with 2-Chloro-1,3,2-dioxaphospholane-2-oxide. The surface was functionalized with DTPA complexes of gadolinium, and the synthesis was carried out first up to generation 2, as shown in Figure 13A. These compounds were used for MR imaging of mice, with a much better contrast enhancement than Magnevist®. They were slowly hydrolyzed at acidic pH, but rapidly hydrolyzed at pH = 7.4 [62]. The synthesis was then carried out up to generation 5 starting from a trifunctional amine core. It was shown that even the largest dendrimers did not accumulate in mice organs, as it could be hydrolyzed *in vivo* and excreted out of the body [63]. As previously shown with PAMAM dendrimers, several functions were grafted to the surface of these biodegradable dendrimers, PEG2000 and PEG2000 functionalized with folic acid for targeting tumors (Figure 13B). This compound outlined the KB tumor in nude mice more clearly than Magnevist® [64]. In another example, the gadolinium complexes were grafted in the internal part of the same family of dendrimers built from a β-cyclodextrin core. The surface was functionalized with both sulfonamides as hypoxia-targeting groups, and zwitterionic groups (Figure 13C). Hypoxia is one of the critical features in solid tumors, thus hypoxia-targeting contrast agents should enhance their specificity. It was shown that this dendrimer greatly enhanced the MRI of orthotopic breast tumor in a mouse model [65].

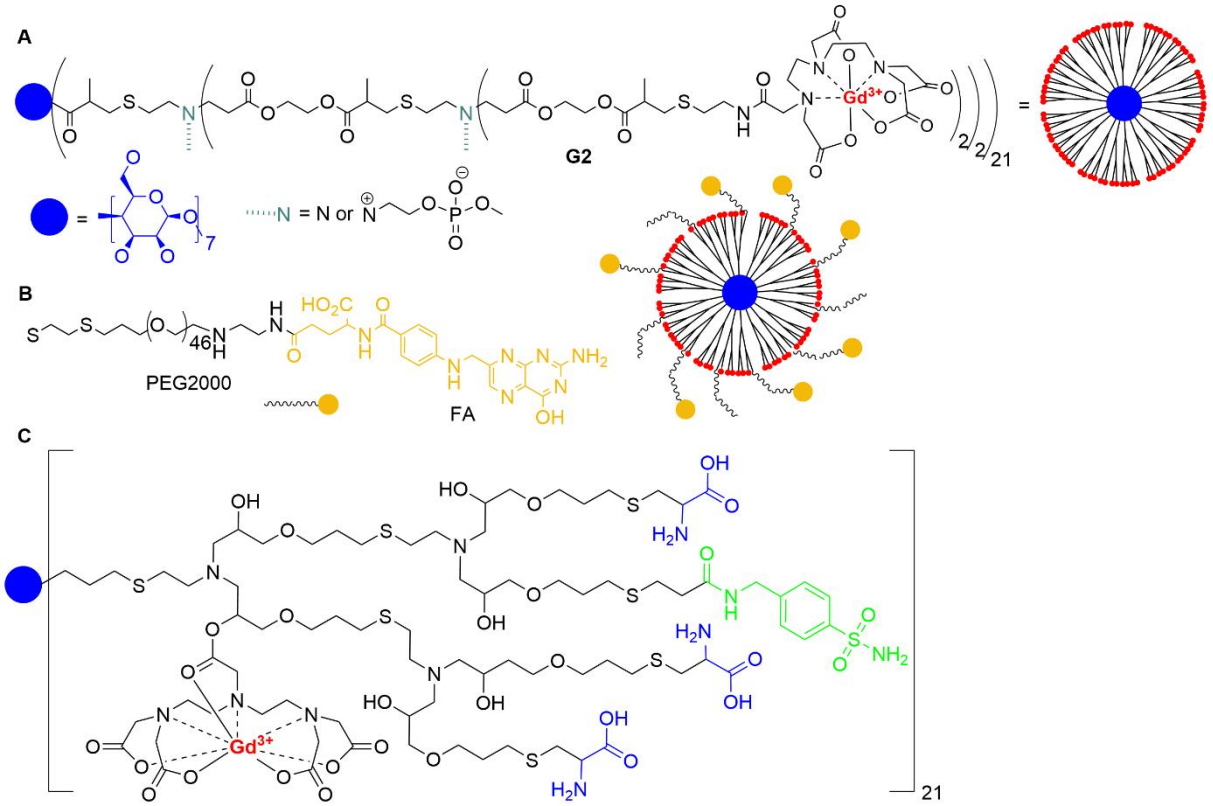

Figure 13. Several dendrimers build from a β-cyclodextrin core bearing DTPA-Gd complexes as either all or some terminal functions.

Two families of anionic linear globular dendrimers (ALGD) based on a polyethyleneglycol (PEG) core and biodegradable polyester dendritic branches on each extremity of the PEG have been synthesized. The first family was based on the multiplication by two of the number of functions at each branching point, whereas the second family was based on a multiplication by three. The third generation of the first family was first functionalized by DTPA on half of the terminal functions, then the targeting cyclic RGD peptide labelled with fluorescein was linked on some DTPA functions, and finally gadolinium was added, and complexed by DTPA (Figure 14A). This compound was used to detect tumor angiogenesis and assess the early response to antiangiogenic therapy in mice [66]. Only the first and second generations of the other examples of anionic linear dendrimers based on a multiplication by 3 at each branching point (Figure 14B) were used as MRI contrast agents. These ALGD were functionalized with C595 monoclonal antibody against breast cancer cell, then Gd was added and complexed with the surface groups of ALGD. Good tumor accumulation and detection were observed in mice xenografted in the right foreleg muscle with 10^6 human breast cancer cells MCF-7. Comparison with commercially available Magnevist®, the monomeric DTPA complex of Gd, showed that the dendrimer Gd-ALGD-G2-C595 afforded MR images with a much better resolution. Furthermore, delayed images obtained 12 and even 24 hrs after i.v. injection still afforded an excellent contrast when using the dendrimer (Figure 14C) [67]. The first generation of this family of ALGD was functionalized with DTPA-Gd complexes and bis(N-methylamine) and used as MRI contrast agents *in vivo* [68]. Recently, the second generation ALGD was functionalized with asparagine (Figure 14B) and used for the ill-defined complexation of gadolinium with the CO_2^- terminal functions. In addition to the contrast agent properties, this compound also displayed remarkable anticancer activity in mice [69].

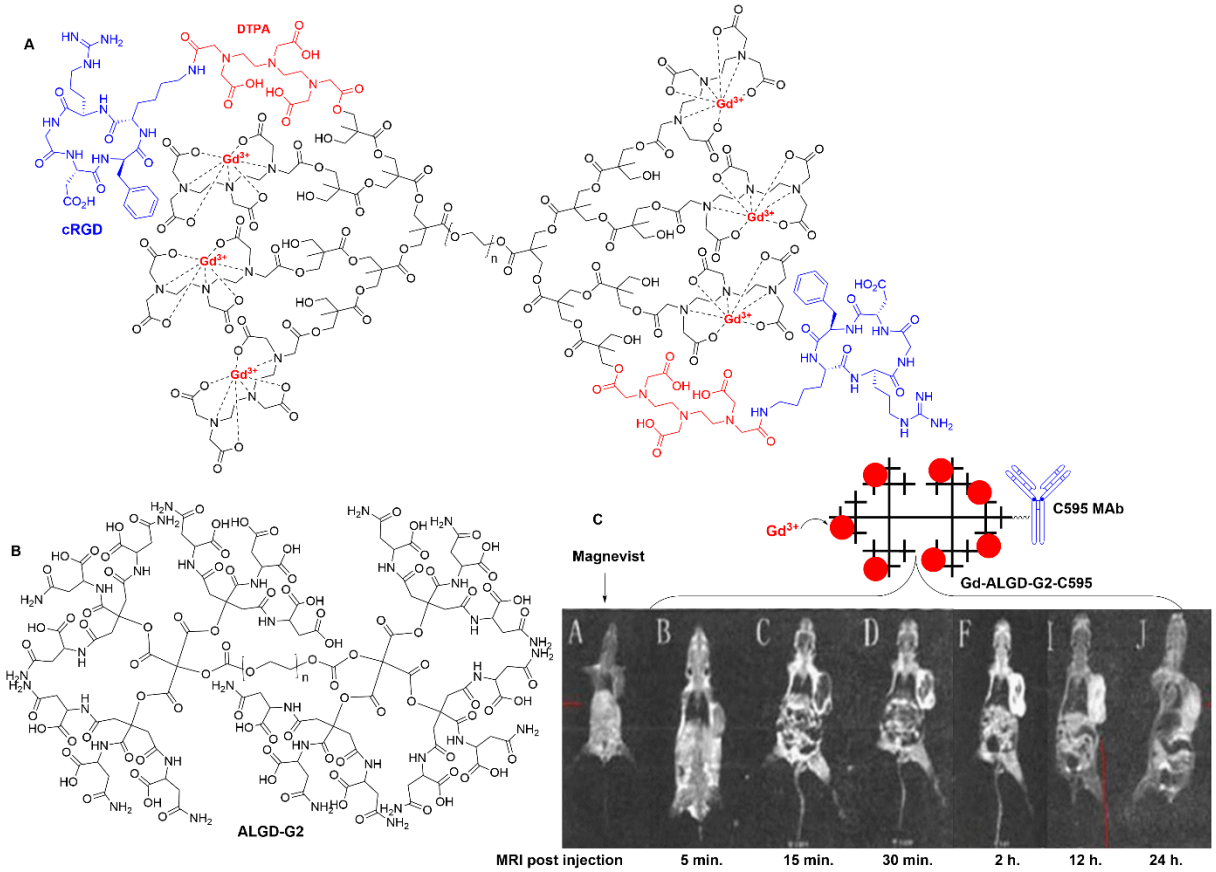

Figure 14. Two examples of anionic linear globular dendrimers (ALGD). Part (C): MR images after i.v. injection of Magnevist (image A) or Gd-ALGD-G2-C595 to mice bearing breast cancer tumor in the fight foreleg muscle (images B-J at different times after injection) (reproduced from ref. 67. Copyright M. Mirzaei et al., open access article).

3.1.5. Macrocyclic Gd complexes of other dendrimers or dendrons

Macrocyclic complexes of Gd were grafted to the surface of dendrimers, but also on the surface of dendrons, and also used as cores of dendrimers. Second and fifth generations of PPI dendrimers were functionalized on the surface with DOTA complexes of Gd, attached through an oligoethylene glycol linker of 6 units (Figure 15A). Both dendrimers were used simultaneously and together with a monomeric complex as contrast agent for imaging a tumor on the paw of a mouse. Monte-Carlo simulations were performed to investigate the multi-agent tracer-kinetic [70]. The fourth generation of the PPI dendrimers were also functionalized with DOTA-Gd complexes, but only on a few terminal functions, the others being functionalized with maltose (Figure 15B). This compound allowed MR imaging of aorta, renal artery, kidney, and bladder of a mouse [71]. Generations 3 and 5 of 1,3,5-triazine dendrimers were functionalized with DOTA complexes (Figure 15C), as they were functionalized with DPTA complexes in Figure 12. Comparison of the MRI properties of DOTA and DTPA Gd complexes indicated that the DOTA complexes afforded higher relaxivity values. Both complexes were used for imaging the whole body of mice [61]. A last example concerns a dendrimer built from a β-cyclodextrin core with polyglyrerol branches, and modified with L-cysteine as terminal functions, together with a few Gd-DOTA complexes (Figure 15D). This compound was compared with G5-PAMAM dendrimers reacted with DOTA-NHS on a few NH_2 terminal functions. It was used for MR imaging of the heart of mice. Interestingly, in contrast to the high Gd retention in liver and spleen with the G5-PAMAM, there was no observable retention in these organs with the polyglycerol dendrimer [72].

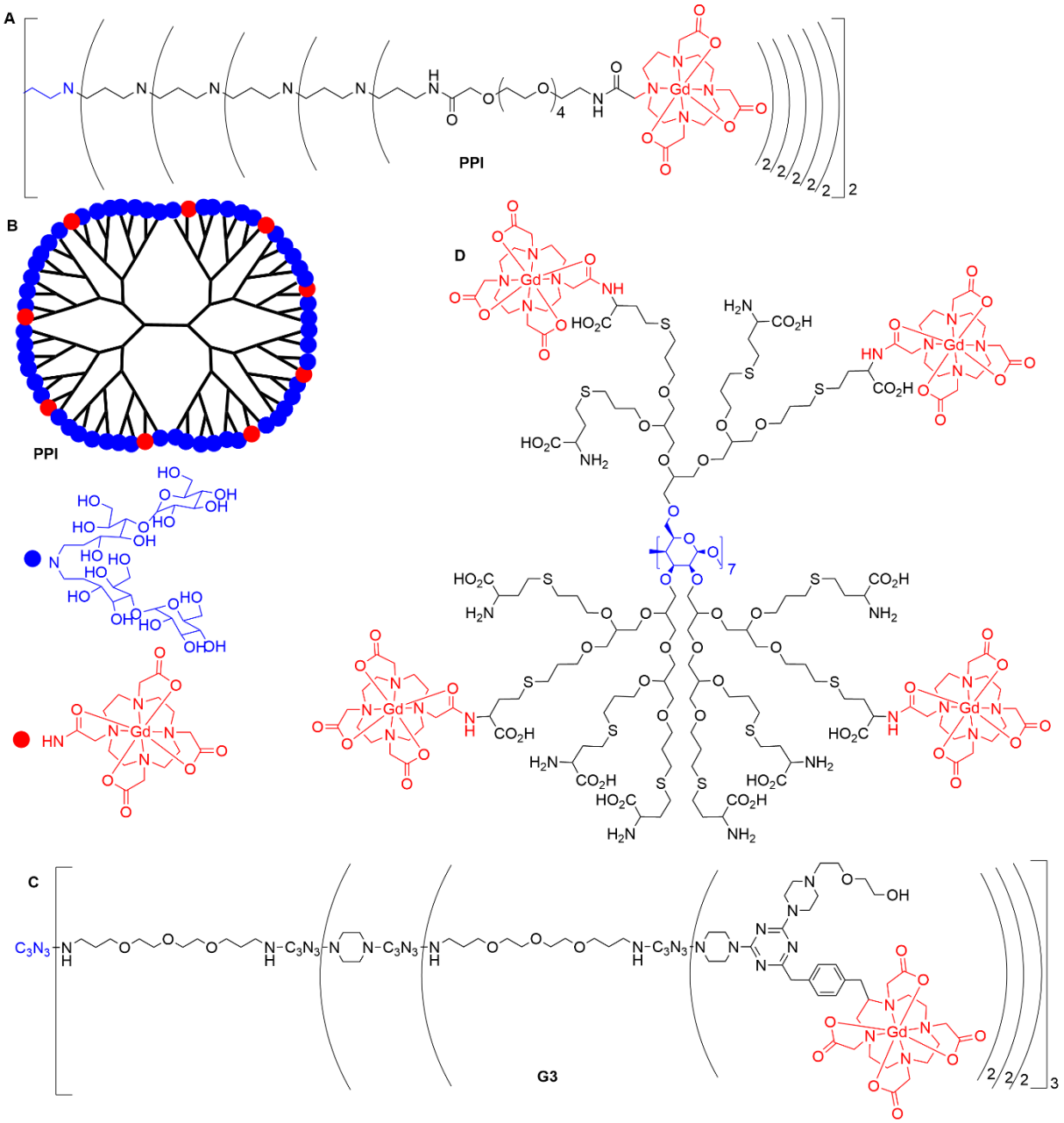

Figure 15. Examples of dendrimers functionalized with DOTA complexes of gadolinium.

In the case of dendrimers built from a macrocyclic core, there is only a single gadolinium per dendrimer, in contrast to all the previous cases. The core is constituted of 1,4,7-triazacyclononane, to which 3 chiral polybenzylether branches are attached, ended by diol groups. This small dendrimer was used for imaging mice. A pharmacokinetic difference was observed between (*R*) and (*S*) optical isomers, the (*S*) isomer being retained in vasculature for longer time than the (R) isomer [73]. The same family of dendrimers was expanded with the synthesis of larger polybenzylether chiral branches of second or third generation (Figure 16). These compounds were used for MR imaging of mice full body, and compared with monomeric Gd-DTPA. Most Gd-DTPA was excreted through the kidneys within 30 min, contrarily to the second and third generation dendrimers. No accumulation was observed in specific organs with the dendrimers. The third generation dendrimers 3-(R) and 3-(S) provided much greater contrast enhancement than the second generation 2-(R) and 2-(S). The (*S*) isomer of the larger dendrimer displays the greatest contrast enhancement in blood [74].

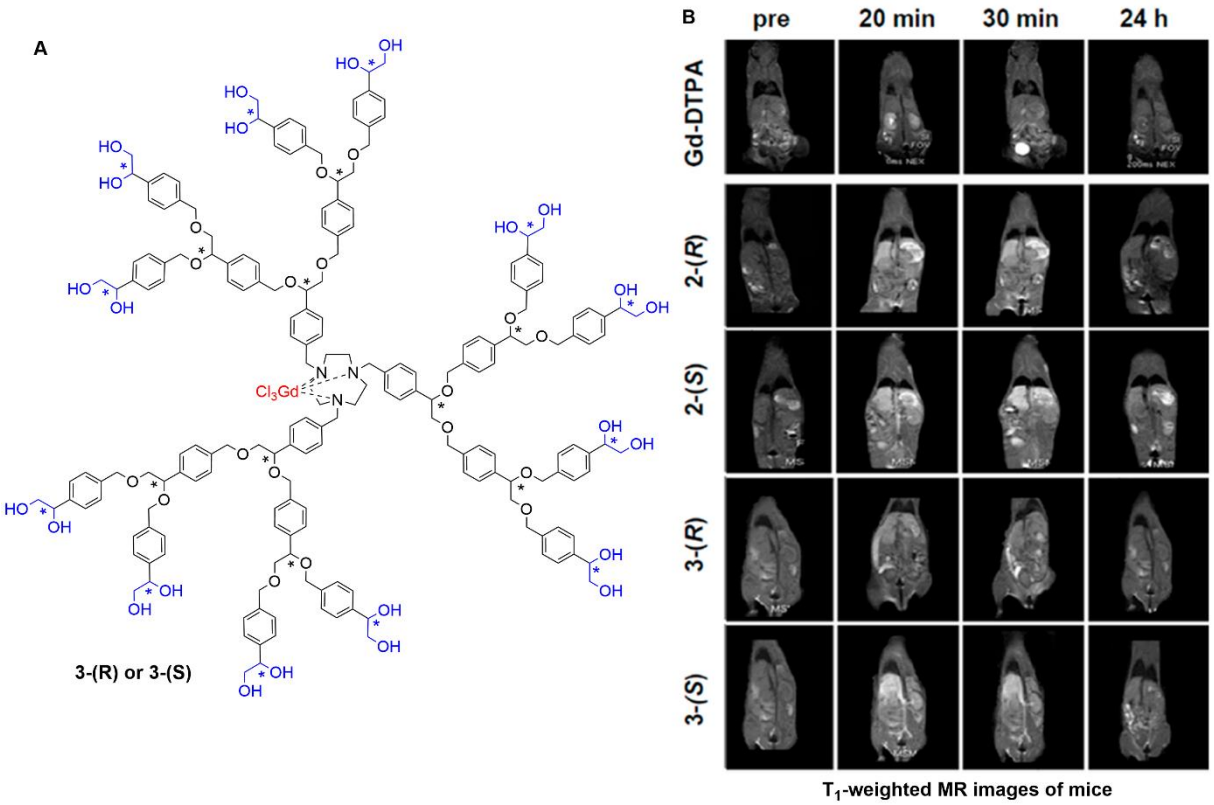

Figure 16. Chiral polybenzylether dendrimer built from a macrocyclic complex of gadolinium at the core (A). Part (B): T_1-weighted MR images of mice before and after intravenous injection of monomeric DTPA-Gd or the cored-dendrimers of generation 2 or 3 (reproduced from ref. 74. Copyright T. Kondo et al., open access article).

Several types of dendrons were also synthesized, and used either alone as imaging agents, or grafted to linear polymers. The nature of the function at the core modifies the properties of the dendrons. In some cases, this function is relatively small, such as a carboxylic acid at the core of amide dendrons functionalized on the surface with 4 DO3A complexes of Gadolinium (Figure 17A). This compound was used to detect tumor in mice transplanted subcutaneously with B16-F10 melanoma cells. Significant contrast enhancement was observed in several organs (vessel, spleen and liver) [75]. A small dendron having at the core a penta-peptide suitable for binding to fibrin–fibronectin complexes that are abundant in the tumor microenvironment of fast-growing breast cancer, and 3 gadolinium complexes on the surface for imaging was synthesized (Figure 17B). This dendron was used for detecting micrometastasis by MRI in female mice bearing metastatic 4T1 breast tumors. The sensitivity of MRI in detecting metastatic tumors was assessed in comparison with fluorescence cryo-imaging, using GFP (green) and Cy5.0 (red) fluorescence (Figure 17B). MRI was able to detect 91% of the GFP-labelled metastases with size >0.5 mm^3 [76].

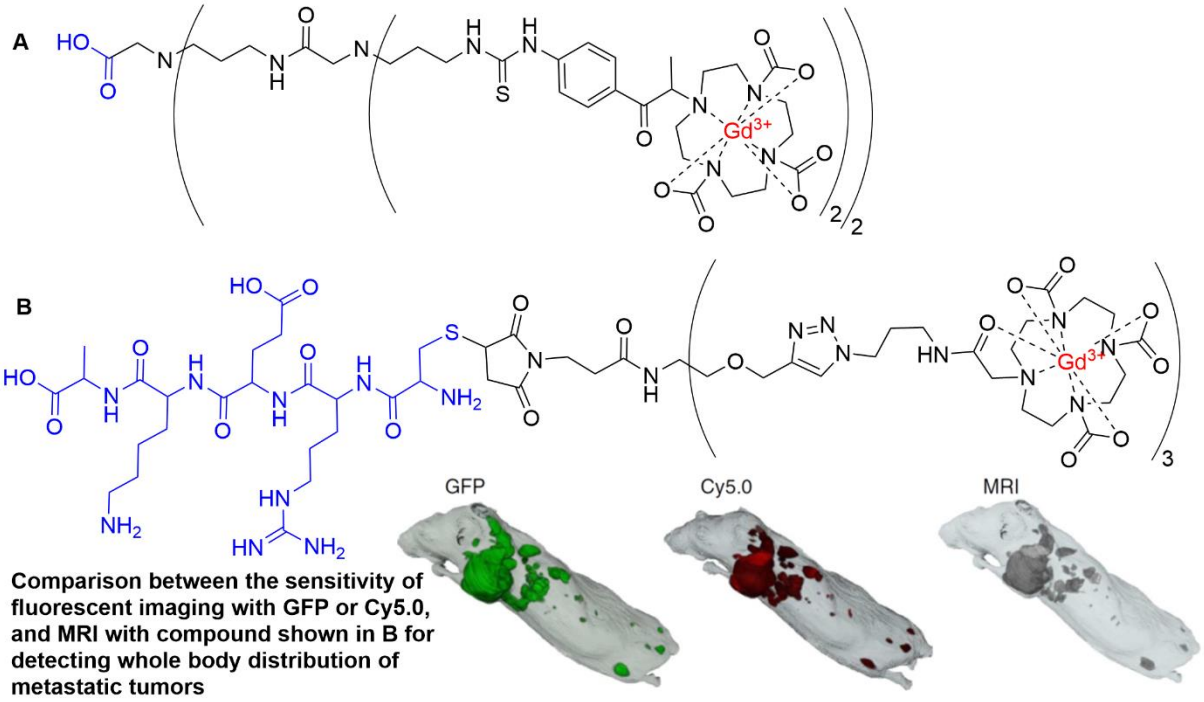

Figure 17. Small dendrons having DO3A gadolinium complexes as terminal groups. Part (B): the small dendron B is used for the detection of metastatic tumors in mice by MRI, and for comparing its efficiency with that of fluorescence (GFP and Cy5.0) (reproduced from ref. 76. Copyright D. Wilson, Z.R. Lu et al., open access article).

In some cases, the function at the core is a long PEG chain (PEG 5K). Three generations (1-3) of gallic acid triethylene glycol dendrons bearing a PEG chain at the core were functionalized on the surface with azides, then used in "click" reactions (azide-alkyne cycloaddition) for the grafting of alkyne-DO3A-gadolinium complexes (Figure 18A). These dendrons were used for imaging a tumor in a mouse brain. The second generation was the most efficient of the three generations [77]. The same PEG derivative was used as core of another dendron, constituted of lysine branches and having on the surface both cholic acid and the porphyrin pyropheophorbide a (Figure 18B). These dendrons form micelles, with the hydrophilic PEG chain in the external part of the micelle. The porphyrins are suitable for the complexation of Gd(III), in the internal part of the micelle. This micelle-like self-assembled dendrons was used for the detection of tumors in transgenic mice with 'spontaneous' mammary cancers [78].

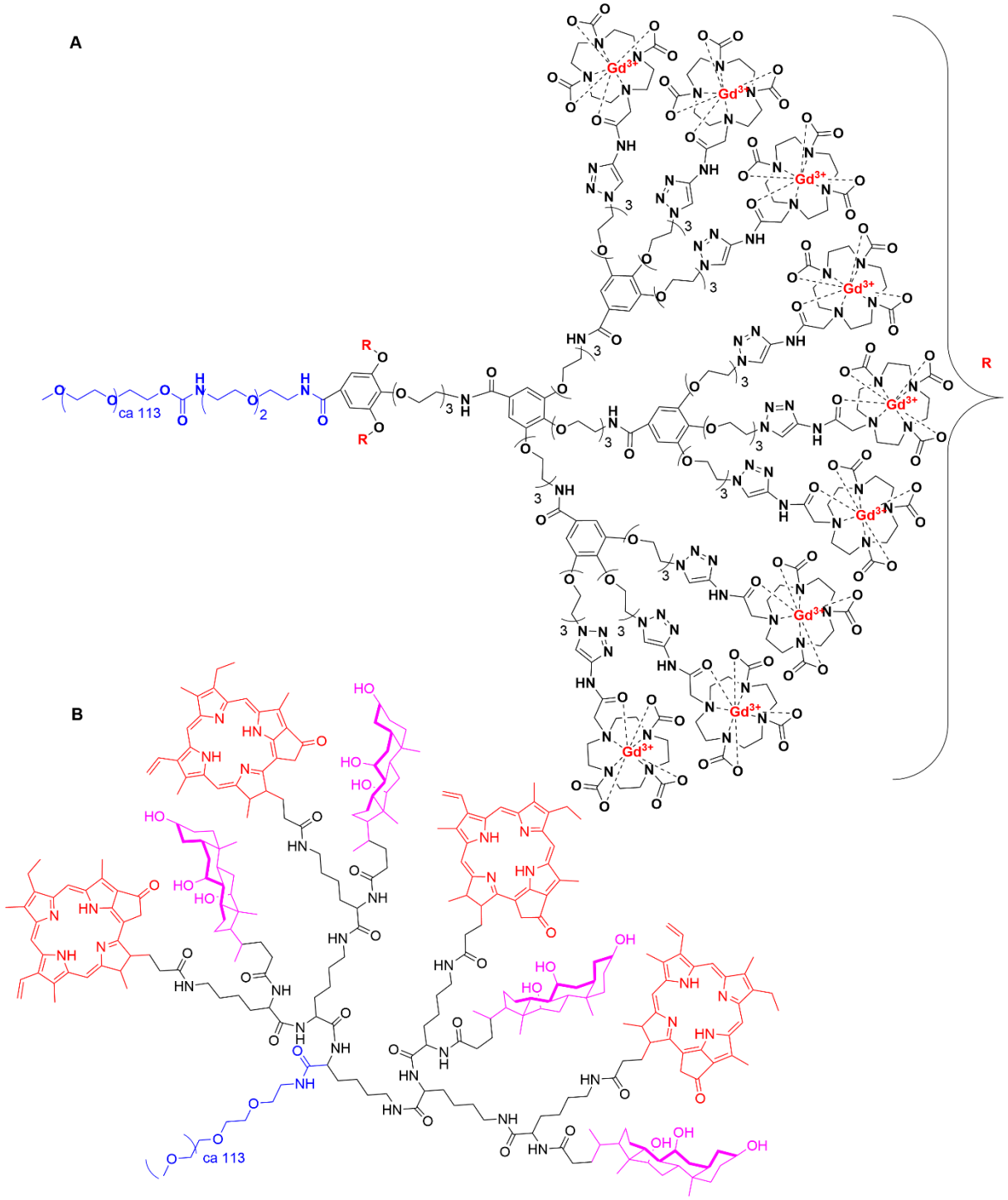

Figure 18. Dendrons bearing a PEG chain at the core and as terminal functions either DO3A-Gd complexes (A) or porphyrin pyropheorbide for the complexation of Gd (B).

Besides long PEG chains, dendrons have been grafted to linear biopolymers. A peptide dendron having gadolinium complexes on the surface and an azide at the core was used in click reaction with heparin partly functionalized with alkynes (Figure 19). Such dendronized heparin was used for MR imaging studies on the mice bearing 4T1 breast tumors, and displayed a high Gd(III) accumulation in the tumor [79]. The same type of peptide dendron was also used in click reactions with hyaluronic acid partly functionalized with alkynes (Figure 19). It displayed a high *in vivo* signal enhancement in 4T1 breast tumors of mice. It was shown that this dendronized biopolymer degraded into products with low

molecular weights in the presence of hyaluronidase, facilitating the elimination and resulting in low Gd residue in the body [80].

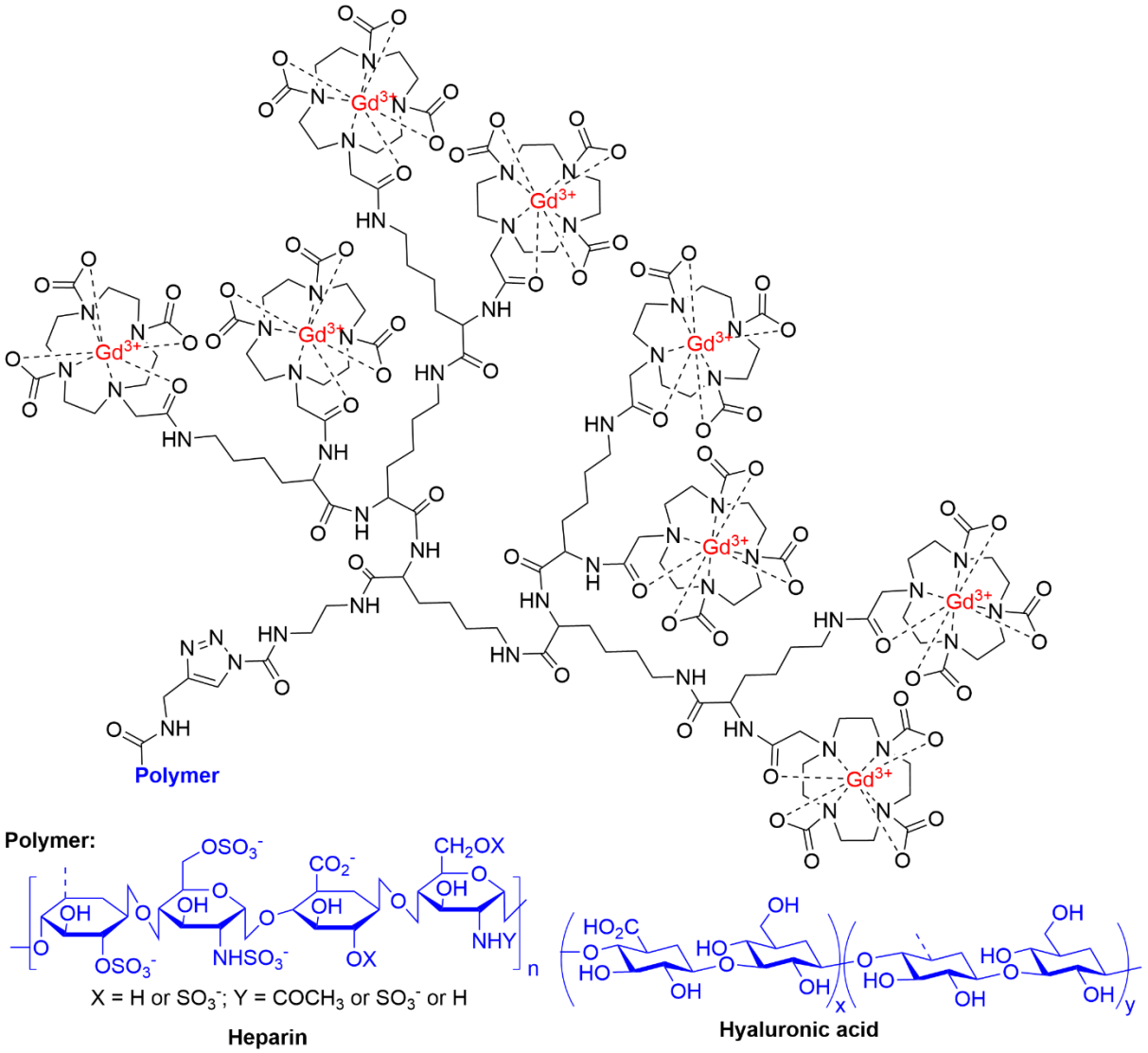

Figure 19. Biopolymers functionalized with dendrons having DO3A-Gd complexes on their surface.

3.2. Dendritic complexes of other metals

Gadolinium has outstanding properties for MR imaging, that is the reason why almost all examples of dendritic complexes used for MRI are based on gadolinium. However, a few other elements can be used also for MRI, and have been complexed with dendritic structures. Ligands used for gadolinium are also suitable for the complexation of other elements. Manganese(II)-NOTA (1,4,7-triaazacyclononane-1,4,7-triacetate) and -DOTA complexes were grafted as terminal groups of dendrimers built from a silsesquioxane core and lysine branches of generations 2, 3, and 4 (Figure 20A). Manganese was chosen as it is much less toxic than gadolinium. The grafting did not occur on all terminal groups, as 23 complexes were grafted to the second generation (instead of 32), 53 for the third generation (instead of 64), and 99 for the fourth generation (instead of 128). These dendrimers are effective for contrast-enhanced tumor imaging in nude mice bearing MDA-MB-231 breast tumor xenografts [81]. Generation 5 PAMAM dendrimer was stochastically functionalized with Mn-DOTA complexes, fluorescein then hyaluronic acid, that can specifically bind to CD44 receptors, a major cell surface marker of progression and metastasis. Then gold nanoparticles were entrapped within this multifunctional dendrimer (Figure 20B). Due to the simultaneous presence of Au-NPs, Mn-complexes and fluorescein, this compound was suitable for computed tomography (CT), MRI, and fluorescence

imaging. It was found efficient *in vivo* for imaging transplanted hepatocellular carcinoma tumors in BALB/c nu/nu male mice. After the tail vein injection of the dendrimer shown in Figure 20B, the CT and MR signal intensity values of the tumors appeared to reach their maxima at 0.5 h post-injection. The CT and MR signal intensity values of the tumors treated with the dendrimer were higher than those of the free HA in the control group at the same time point (Figure 20C) [82].

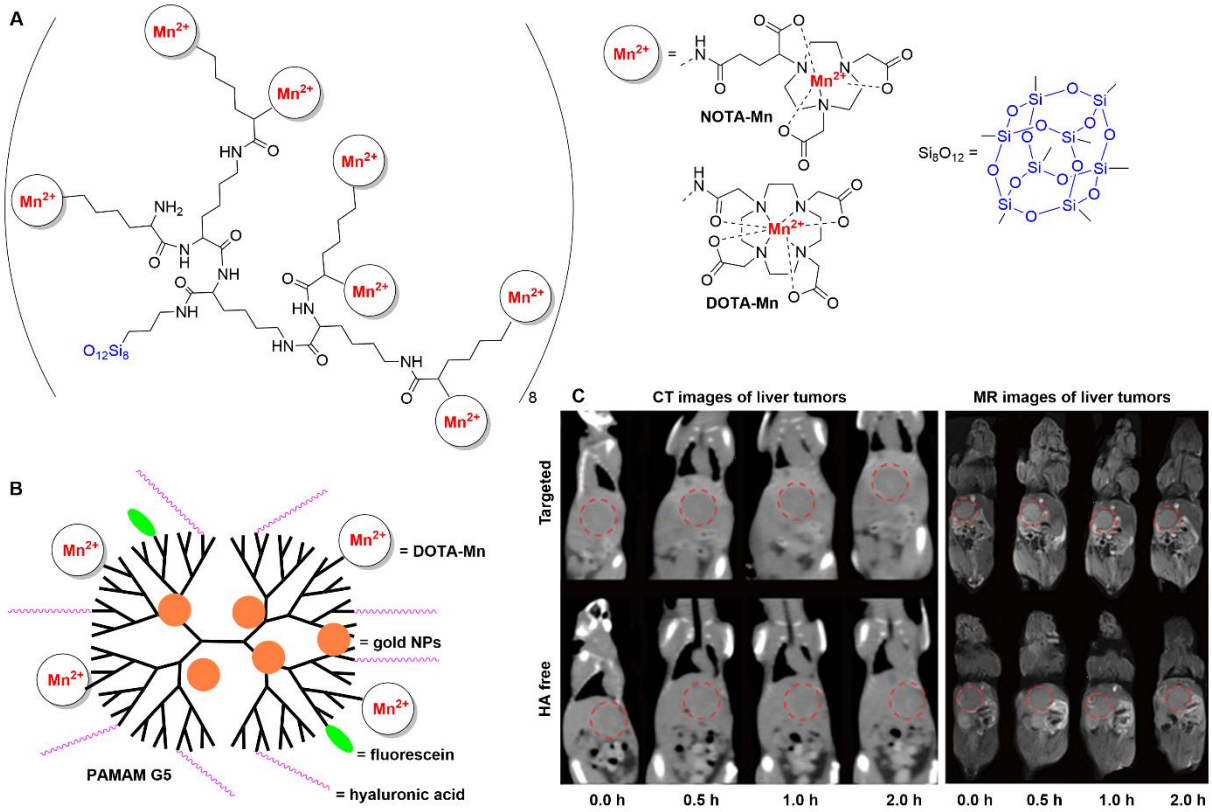

Figure 20. DOTA and NOTA dendritic complexes of Manganese. Part **C**, CT and MR images obtained with the compound shown in **B**, functionalized (targeted) or not (HA free) with hyaluronic acid (reproduced from ref. 82. Copyright R. Wang, Y. Luo et al., open access article).

Besides classical MRI techniques, other techniques such as chemical exchange saturation transfer (CEST) and paramagnetic CEST (PARACEST) offer unique MRI properties. CEST magnetic resonance imaging (MRI) relies on exchangeable protons that resonate at a chemical shift that is distinguishable from the bulk water signal [83]. Europium complexes have been used for such purpose. A G5 PAMAM dendrimer was labelled with the tetraglycineamide derivative of DOTA (DOTAM-Gly) complexing europium; an average of 42 complexes per dendrimer were grafted. The DOTAM-Gly complexes can be linked to the dendrimer through several reactions of the carboxylic acids with the NH_2 terminal functions. Then the fluorophore DyLight 680 NHS was reacted on some of the remaining NH_2 functions of PAMAM dendrimers; an average of 1 DyLight 680 per dendrimer was grafted (Figure 21). This compound enhanced the detection by CEST MRI of a tumor in the brain of an athymic nude rat having a U87 human glioma tumor [84,85].

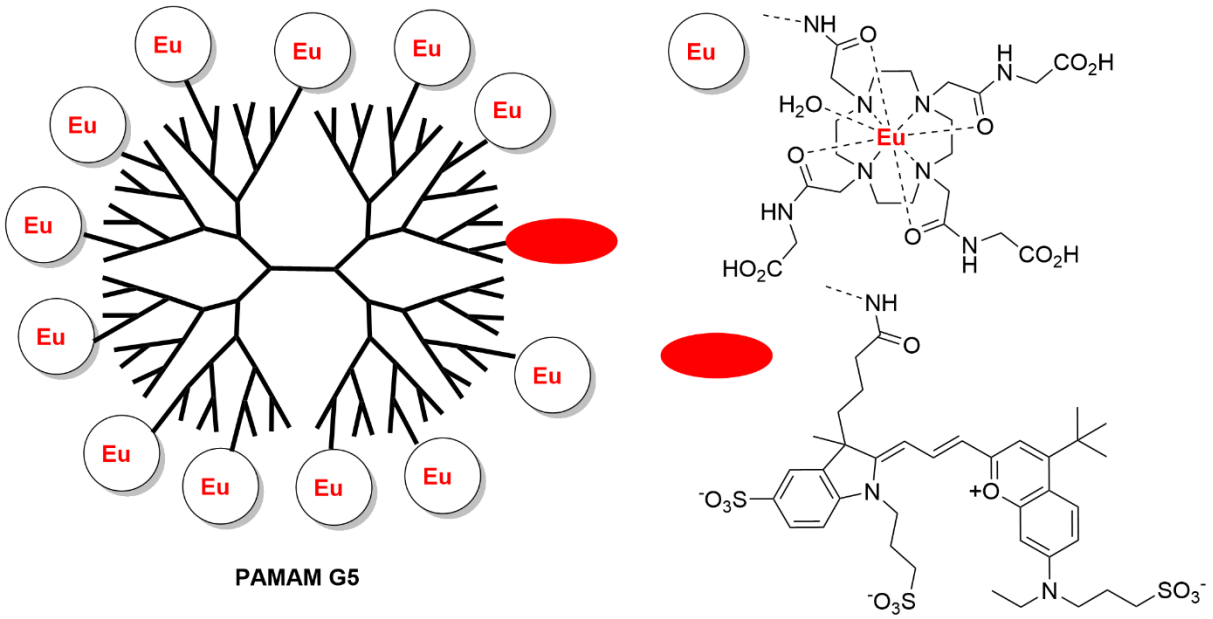

Figure 21. PAMAM dendrimers functionalized with DOTA europium complexes and DyLight 680. Only one isomer is shown.

4. Radioactive dendrimer complexes for SPECT imaging

Radiopharmaceutical drugs are used routinely in nuclear medicine for the diagnosis and/or the therapy of various diseases. In this review, we will consider only the diagnosis aspect. Two different imaging techniques using radionucleides are of clinical relevance: Single Photon Emission Computed Tomography (SPECT), and Positron Emission Tomography (PET). They differ by the type of emission of the radioisotope, and in the energy range. SPECT uses γ-emitters in the energy range 75-360 keV, with radionucleides such as ^{99m}Tc, ^{67}Ga, ^{111}In, ^{123}I, ^{153}Sm or ^{177}Lu. For PET, the energy of positron emitting isotopes is variable, but all generate by annihilation two 511 keV photons; the PET image is based on the secondary emission of the γ-photons. PET uses generally lighter elements than SPECT, such as ^{13}N, ^{15}O, ^{18}F, ^{64}Cu, ^{68}Ga, ^{86}Y, ^{89}Zr, but also ^{124}I. The very high sensitivity of such techniques allows the use of very low concentrations of radionucleides, from 10^{-6} to 10^{-8} M. The field of radioactive dendrimers has been early reviewed [86], and more recently [87], on precise topics such as PET [88], or radioactive PAMAM dendrimers [89]. However, none of these reviews focused on radioactive complexes, which will be the topic of the next paragraphs. Covalent grafting, which is most generally the case of iodine for instance, will not be considered in this review, only complexes.

4.1. Dendritic complexes of Technetium

The metastable isotope ^{99}technetium is the most widely used radionucleide, due to its half-life of 6h, and its suitable gamma emission of 140 keV [90]. As already observed with gadolinium, the complexation of technetium has been essentially carried out with DTPA and sometimes with DOTA ligands stochastically grafted on the surface of PAMAM dendrimers.

4.1.1. Technetium complexes of PAMAM dendrimers

An attempt has been made to complex technetium only by the structure of a generation 4 PAMAM dendrimer, bearing a few fluorescein labels without additional ligands. This association was used for scintigraphy imaging studies of melanoma-bearing mice [91]. However, in most cases a ligand is needed for the stable complexation of ^{99m}Tc. For instance, a generation 5 PAMAM dendrimer was first partially acetylated (ca 81 acetyl groups), then functionalized with biotin and DTPA. This compound was either directly labelled with ^{99m}Tc (Figure 22A) or was conjugated with avidin, and finally ^{99m}Tc was complexed. Both compounds were tested first *in vitro*, and the avidin conjugate was found more stable, thus it was used for micro-SPECT imaging of mice. The highest uptake was observed in liver and

spleen [92]. A generation 4 PAMAM dendrimer bearing 64 terminal amines was partially acetylated (35 acetyl groups) with sulfosuccinimidyl acetate, then 2,3,5-triiodobenzoic acid (TIBA) was coupled to 64% of the remaining NH_2 functions, resulting in ca 15 TIBA (radio-opaque agent) per dendrimer. Then ca 4 p-SCN-Bn-DTPA were grafted, followed by PEG (12 CH_2CH_2O units) grafted on all the remaining NH_2 functions (ca 10), and finally ^{99m}Tc was complexed by the DTPA derivatives (Figure 22B). This dendrimer was used for both SPECT and X-ray computed tomography (CT) imaging of healthy wild-type C57BL/6 mice. Such association offers a great advantage for image processing and quantification, to gain information regarding anatomical structure and physiological function, such as absolute myocardial blood flow [93].

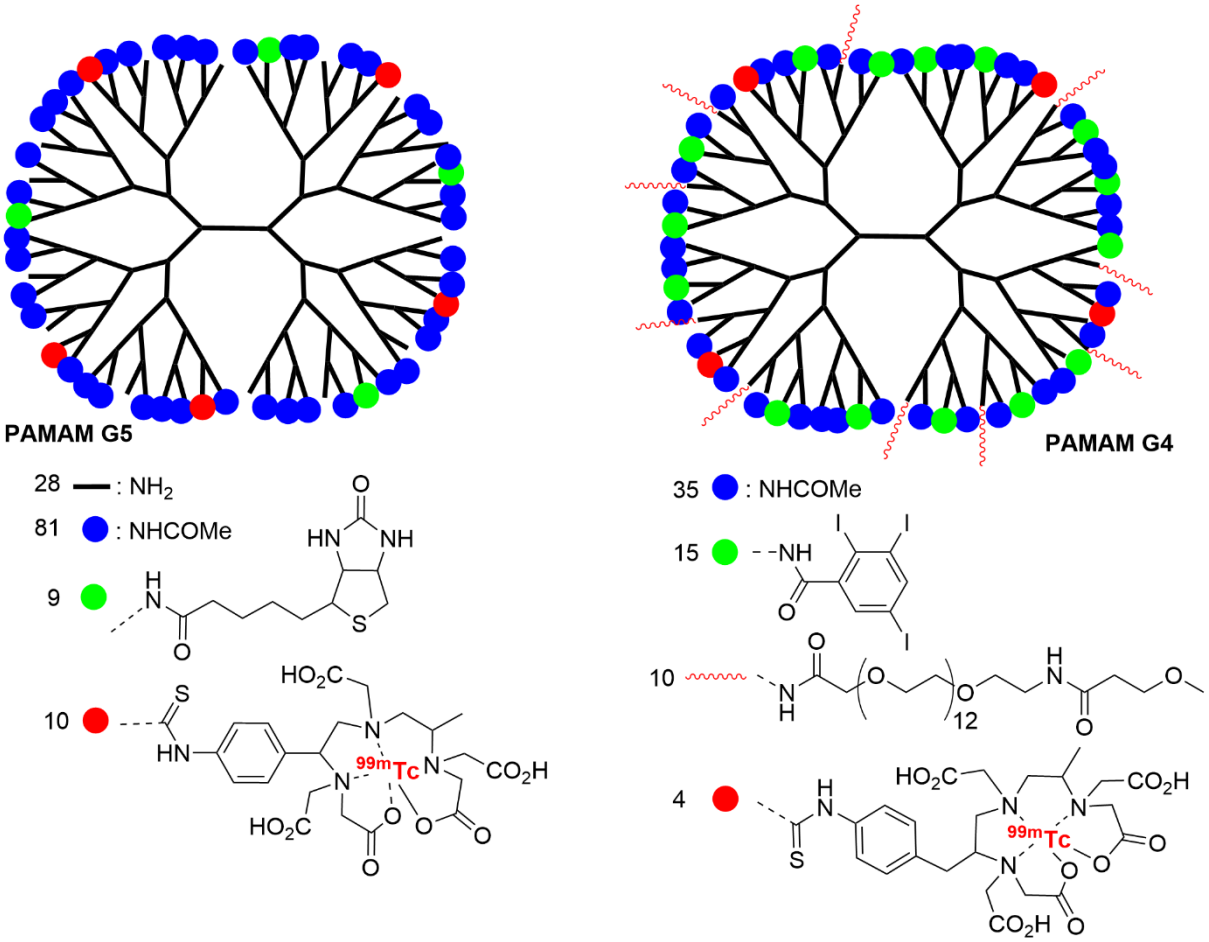

Figure 22. Multifunctionalized PAMAM dendrimers bearing DTPA-^{99m}Tc complexes on their surface for SPECT experiments. Only one isomer is shown.

The second generation PAMAM dendrimer was also used as support of several types of functions, and associated with gold nanoparticles, for SPECT/CT dual mode imaging. In a first example, the dendrimer was functionalized with ca 3 DTPA via an amide linkage, then with ca 7 folic acids via a PEG spacer (MW 2000) for targeting tumors. This compound was used as template for the synthesis and encapsulation of gold NPs, and finally ^{99m}Tc was complexed by DTPA (Figure 23A). This compound was injected to mice bearing a subcutaneous xenografted tumor model. A dual mode of micro-SPECT/CT was used, where CT was used to localize the animal skeleton and bones. A high SPECT signal intensity was measured in the tumor [94]. An analogous work was carried out with the FC131 cyclic peptide (a CXCR4-specific ligand, which is overexpressed in glioma) instead of folic acid on the end of the PEG linkers (Figure 23B). This multifunctionalized G2 PAMAM dendrimer appeared effective in targeted SPECT/CT imaging of glioma cells *in vivo* in mice bearing a subcutaneous tumor model [95]. The second generation PAMAM was also functionalized with NOTA (triazanonane macrocycle) for the complexation of ^{99m}Tc, and with the RGD cyclic peptide (arginine-glycine-aspartic acid) on the end of

the PEG linkers (Figure 23C). This compound entrapping gold NPs was used as nanoprobe for targeted SPECT/CT dual mode imaging of a C6 tumor (glyoma cells) in mice [96]. The fifth generation PAMAM dendrimer was also used in connection with gold NPs. This dendrimer was functionalized with PEGs and ^{99m}Tc DTPA complexes, and the other functions were either acetyl of hydroxyl groups (Figure 23D). The biodistribution profile of these compounds, as detected by SPECT/CT images, was significantly impacted by the presence of the acetyl/hydroxyl groups. The acetyl dendrimer was mainly detected in the lung, whereas the hydroxyl dendrimer was mainly detected in the blood (heart, kidney, and postcaval vein) [97].

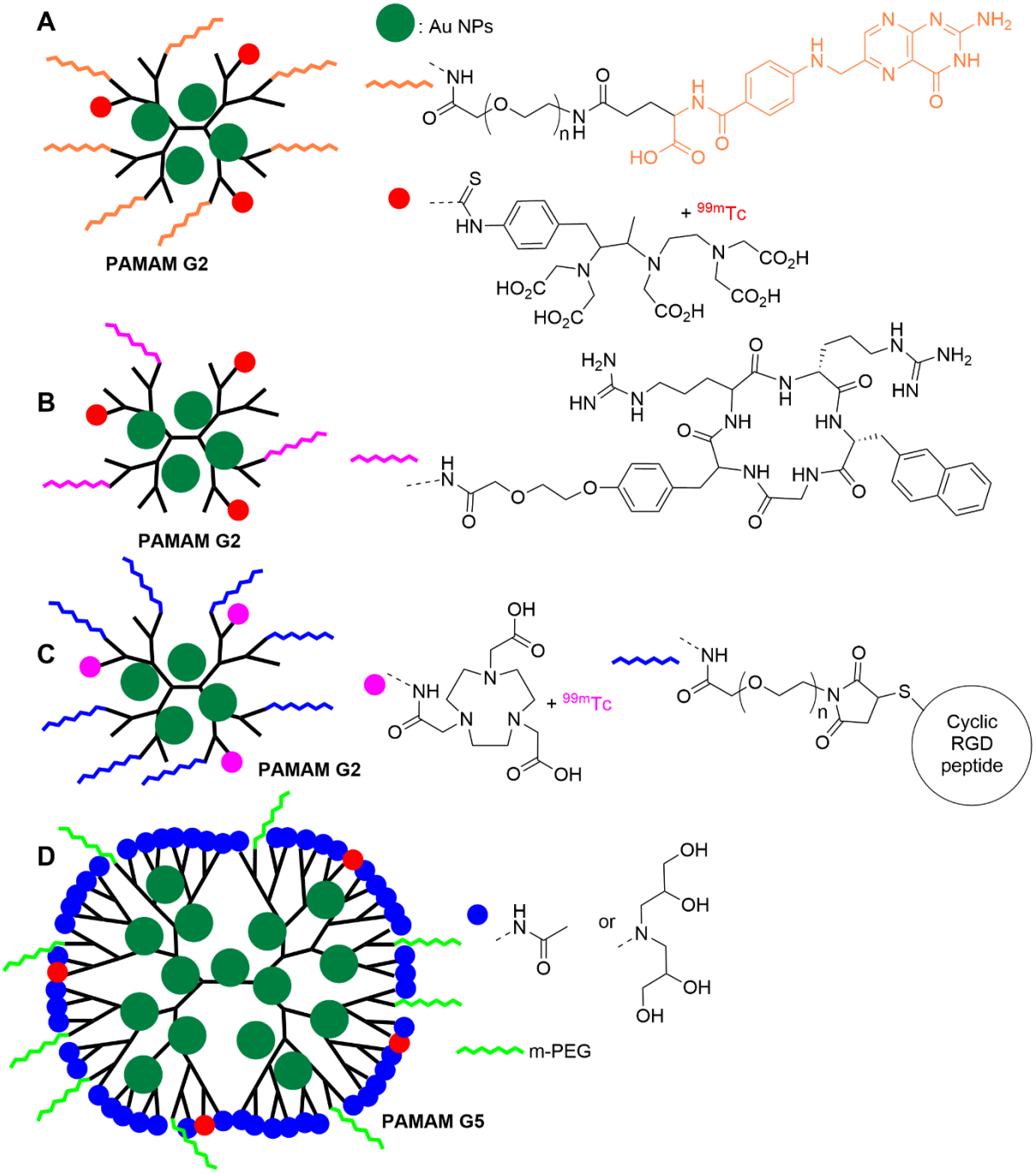

Figure 23. Generations 2 and 5 of PAMAM dendrimers, functionalized with DTPA or NOTA complexes of ^{99m}Tc and other functions, and incorporating gold nanoparticles in their structure for dual imaging.

A few other types of ligands for ^{99m}Tc have been grafted on the surface of PAMAM dendrimers. The generation 5 was functionalized with folic acid, fluorescein and DOTA chelators. These chelators were

used for the complexation of both Mn for magnetic resonance imaging and ^{99m}Tc for SPECT imaging (Figure 24A). Both methods allowed to detect the presence of a tumor in a xenografted tumor model of BALB/c nude mice [98]. The generation 4 was functionalized with mPEG, folic acid, and succinyl hydrazinonicotinic acid (suc-HYNIC), as original ligand for the chelation of ^{99m}Tc together with tricine (N-tris-(hydroxymethyl)-methylglycine) as additional ligand. This dendrimer was then loaded with 5-fluorouracyl, an anticancer drug (Figure 24B). Female BALB/c mice injected with breast carcinoma 4T1 cells, received two weeks after the dendrimer. A specific localization of the dendrimer at the tumor site was observed, but also an accumulation in the liver and spleen [99]. The generation 3 PAMAM was functionalized with folate and also with 2-hydrazinonicotinic acid for the complexation of ^{99m}Tc, with tricine and trisodium triphenylphosphine-3,3′, 3″-trisulfonate as co-ligands (Figure 24C). SPECT/CT imaging was successfully performed with this dendrimer injected to mice bearing a KB tumor [100].

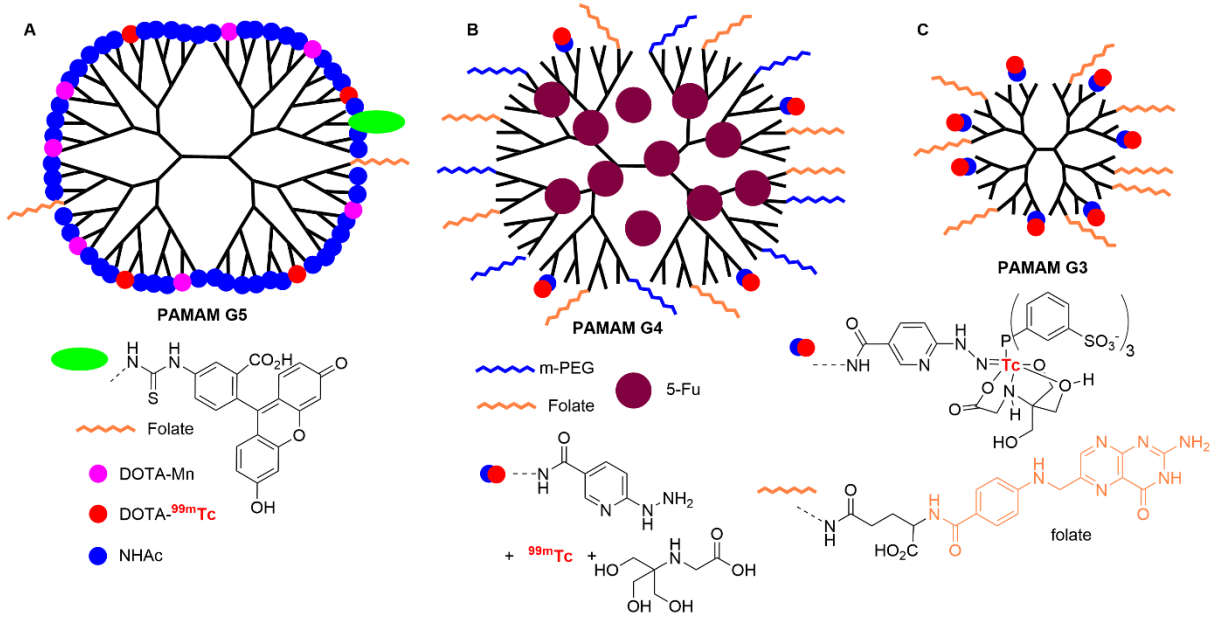

Figure 24. Generations 5, 4, and 3 of PAMAM dendrimers functionalized by folate and by complexes of ^{99m}Tc. (A) DOTA complexes; (B and C) Hydrazinonicotinic acid and tricine complexes.

4.1.2. Technetium complexes of other dendrimers

Besides PAMAM dendrimers, a few examples of polyester dendrimers used for the complexation of ^{99m}Tc have been published. An example concerns a fifth generation of aliphatic polyester dendrons having a dipicolylamine chelate for ^{99m}Tc at the core, and three different molecular weight mPEGs (mPEG160, mPEG350, and mPEG750) grafted to the surface by thiol-ene click chemistry (Figure 25A). This compound was used for SPECT imaging studies of healthy rats, then of H520 (human lung squamous cell carcinoma) xenograft in CD1 nu/nu mice tumor models [101]. The other examples of polyester dendrimers are based on the anionic linear globular dendrimers (ALGD) of second generation shown in Figure 14B. The surface was modified, but not with specific ligands, for the complexation of ^{99m}Tc. These compounds were functionalized with L-methionine; it was estimated that each 100 µg of ALGD conjugate contained approximately 23 µg of methionine (Figure 25B). This modified dendrimer was incubated with ^{99m}Tc, and the resulting complex was used for imaging by SPECT scintigraphy Balb/c mice grafted with HT29 tumor cells [102]. An analogous work was carried out using glucosamine instead of methionine for the surface functionalization (Figure 25C). After incubation with ^{99m}Tc, the complex was also used for SPECT scintigraphy of normal and infarcted rabbits. It was shown in particular that this compound is able to accurately diagnose myocardial infarctions at early stages [103]. For increasing the detection of the cardiac ischemic region, a specific peptide was elaborated and grafted to the ALGD, with no additional functions (Figure 25D). After incubation with ^{99m}Tc, the complex was used for imaging rats, and displayed a high uptake in the cardiac ischemic region [104].

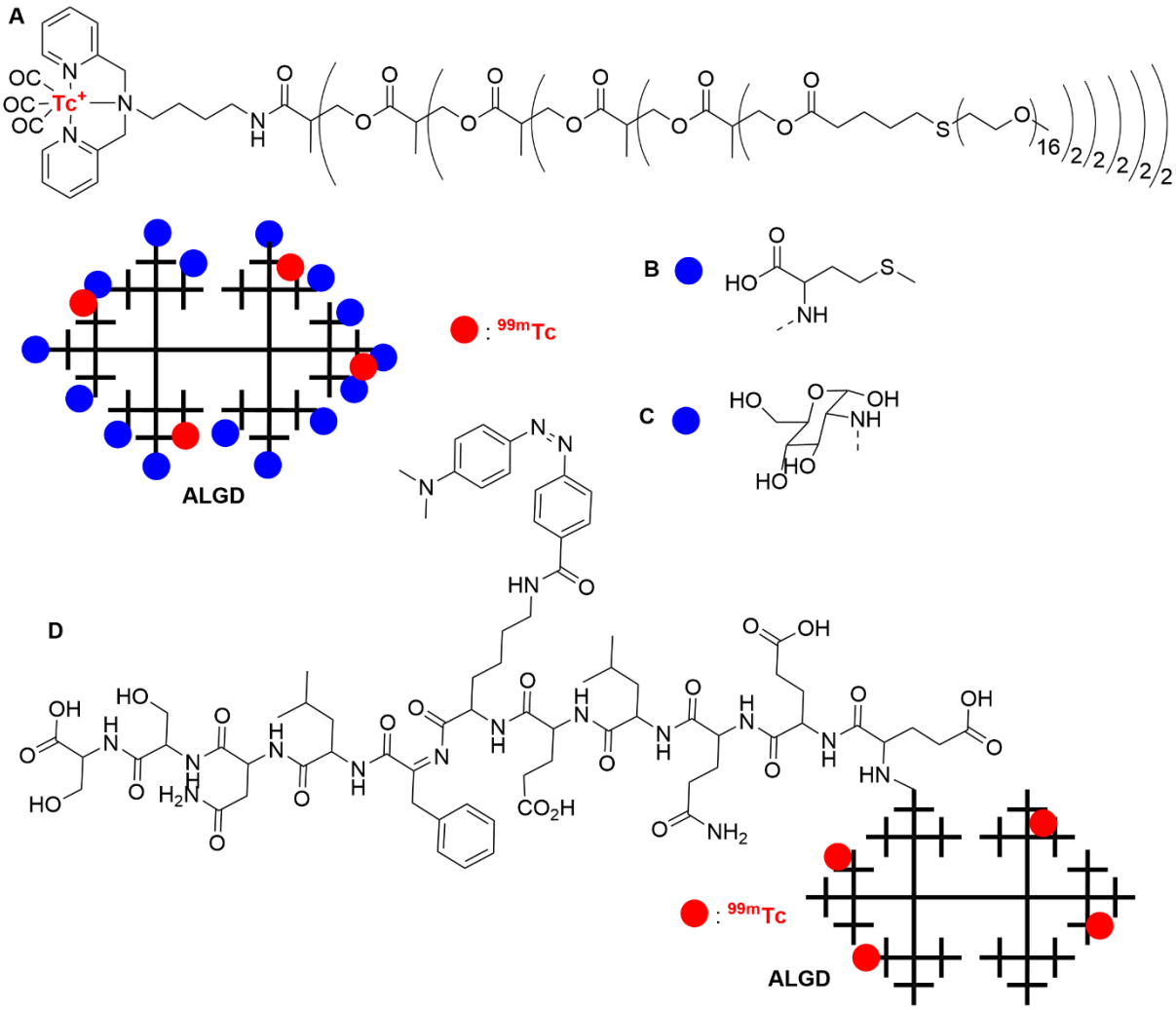

Figure 25. Polyester dendrimers for the complexation of ^{99m}Tc. See the structure of ALGD in Figure 14B.

4.2. Dendritic complexes of radioactive ^{111}Indium

Besides ^{99m}Tc, the other widely used radioelement is ^{111}Indium, which has been mainly associated with different generations of PAMAM dendrimers. ^{111}In is a γ-emitter (as ^{99m}Tc), with a half-life of 67.2 h (to be compared with 6 h for ^{99m}Tc). Generations 1 and 4 of PAMAM dendrimers were conjugated with a bifunctional pyridine-N-oxide DO3A ligand, and used for complexing ^{111}In (Figure 26A). Pharmacokinetic studies carried out with rats demonstrated that the first generation was rapidly eliminated from the body, whereas a long-term accumulation of the fourth generation was observed in the liver and kidney [105]. In order to determine the influence of the tridimensional structure, PAMAM dendrimers were compared with linear poly(glutamic acid). The linear polymer was functionalized with pendant DTPA derivatives. PAMAM G4 acetylated dendrimers and collagen peptide (2kDa)-conjugated dendrimers were also functionalized with respectively 20 and 23 DTPA per dendrimer (among 64 terminal functions) (Figures 26B and 26C). These three compounds were labelled with ^{111}In and injected intravenously into tumor-bearing mice. SPECT images indicated that the linear polymer and the acetylated dendrimers were detected primarily in the kidney and the bladder; the polymer accumulated gradually in the liver, whereas the dendrimer was excluded from the body. In contrast, the peptide dendrimer accumulated in the liver. Subcutaneous injection directly inside the tumor induced a long-term retention inside the tumor for both the polymer and dendrimers [106]. PAMAM G4 was also functionalized with DTPA for the complexation of ^{111}In, and with polyethylenimine and γ-polyglutamic acid in a theoretical charge ratio carboxyl groups of DTPA-G4/nitrogen of PEI/carboxyl groups of γ-PGA of 1:8:16, to get a negatively charged compound (Figure 26D). SPECT imaging using this compound injected to rats indicated a significant accumulation in the popliteal

(sentinel) lymph node [107]. PAMAM G3 was modified with ca 32 L-serine (all the terminal functions, Figure 26E), as a potent renal targeting drug carrier; the corresponding generations 2 and 4 were also synthesized. Various other derivatives such as L-threonine and L-tyrosine were also used to modify the G3 PAMAM dendrimer. All these dendrimers were labelled with ^{111}In and injected to mice. The G3 dendrimer modified with L-serine specifically accumulated in the kidney (82% of the total dose) [108]. The G3 PAMAM was also modified with a mixture of L-cysteine and L-serine (cysteine content 20 or 40%), as a kidney-targeting reactive oxygen species (ROS) scavenger to help prevent renal ischemia/reperfusion injury, and then labelled with ^{111}In. These compounds specifically accumulated in mouse kidney [109]. An S-nitrosylated L-serine-modified PAMAM dendrimer was synthesized as a kidney-targeting NO donor. Indeed, nitric oxide (NO) deficiency is known to play a role in renal ischemia/reperfusion injury. Labelling this dendrimer with ^{111}In permitted to demonstrate that it specifically accumulated in the renal cortex after injection to mice [110].

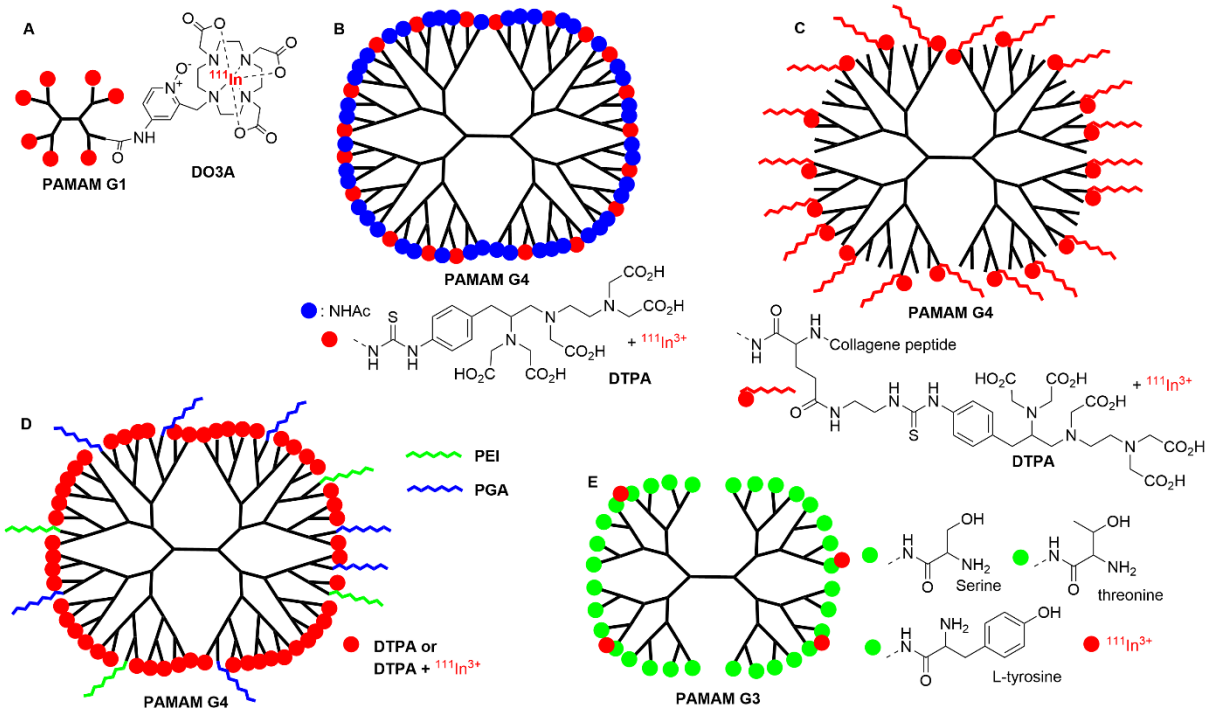

Figure 26. PAMAM dendrimers for the complexation of ^{111}In with DO3A or DTPA.

Almost all examples of dendritic ^{111}In complexes were based on PAMAM dendrimer, but a small dendron was used to synthesize a tetramer which is a peptide antagonist for the chemokine receptor 4 (CXCR4) that is overexpressed in 23 types of cancer. This dendritic tetramer was also functionalized at the core with a Cy5.5-like fluorophore and a DTPA chelate for the complexation of ^{111}In (Figure 27), enabling a multimodal imaging by fluorescence and SPECT/CT. The corresponding monomers and dimers were also synthesized. Mice bearing CXCR4-positive mouse tumor lesions were injected with these dendritic structures. The tumor could be visualized with the 3 compounds (monomer, dimer, tetramer), but the dimer gave better results than the monomer, and slightly better results than the tetramer [111].

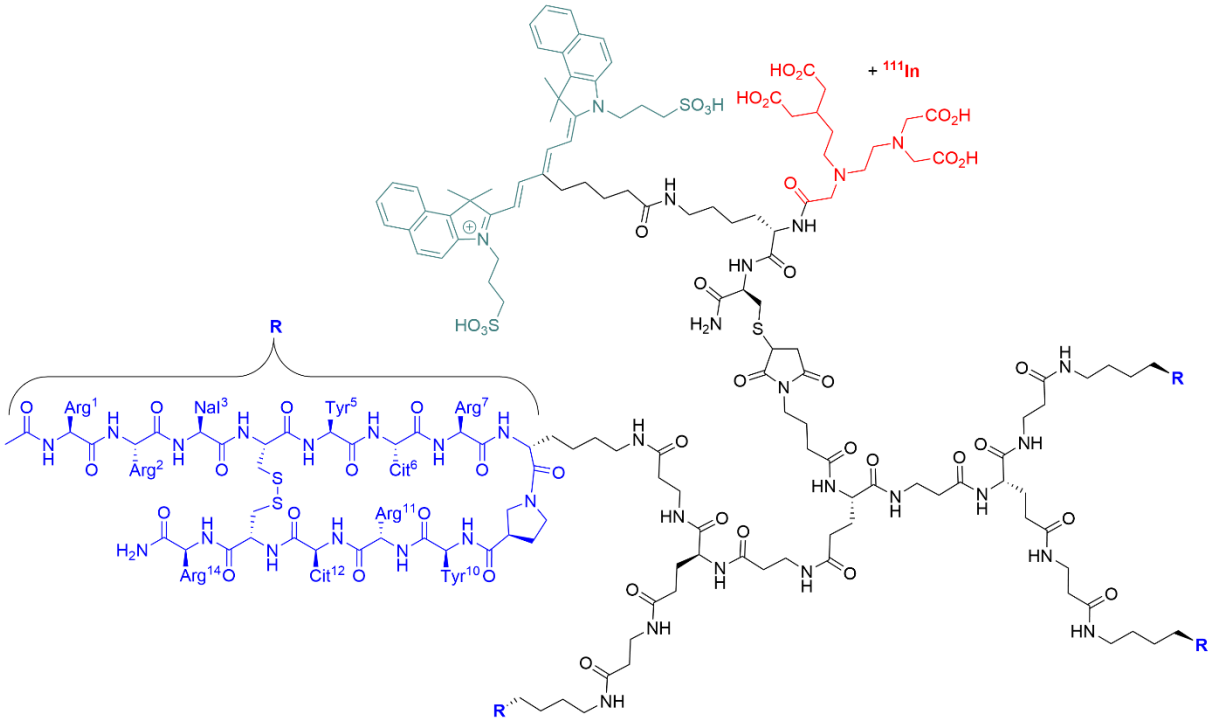

Figure 27. A dendritic tetramer with a Cy5.5-like fluorophore and a DTPA chelate at the core for the complexation of ^{111}In.

4.3. Dendritic complexes of other radioactive elements

A few radioactive versions of gadolinium complexes used for MRI have been synthesized. For instance, in the gadolinium complex shown in Figure 4B, a few ^{153}Gd ions were introduced, but not for imaging [35]. The third generation PAMAM dendrimer was functionalized with DOTA on most of the terminal functions. Then, a very few numbers of remaining NH_2 functions were modified to enable the grafting of trastuzumab, a human monoclonal antibody that can specifically interact with HER-2 (a receptor overexpressed in some breast cancers). The DOTA ligands were used for the complexation of ^{147}Gd radionuclide, and also ^{153}Gd (Figure 28A). These dendrimers are potentially usable as SPECT-MRI molecular imaging agents [112]. A generation 4 PAMAM dendrimer was functionalized with two targeting functions and DOTA for the complexation of ^{177}Lu on the surface, and used for the entrapment of gold nanoparticles in the internal cavities. The targeting functions were the folate, for which cancer cells have a high requirement to maintain DNA synthesis, and a bombesin peptide, for which a receptor is present in 96% of breast cancer tissues (Figure 28B). This dendrimer was injected inside the tumor to mice bearing T47D breast cancer tumor in the upper back. Whole imaging of the body was performed with an optical/X-ray imaging system. Images were taken after 1h or 96h (Figure 28C). It was shown that the optical imaging correlated well with the radionuclide decay [113].

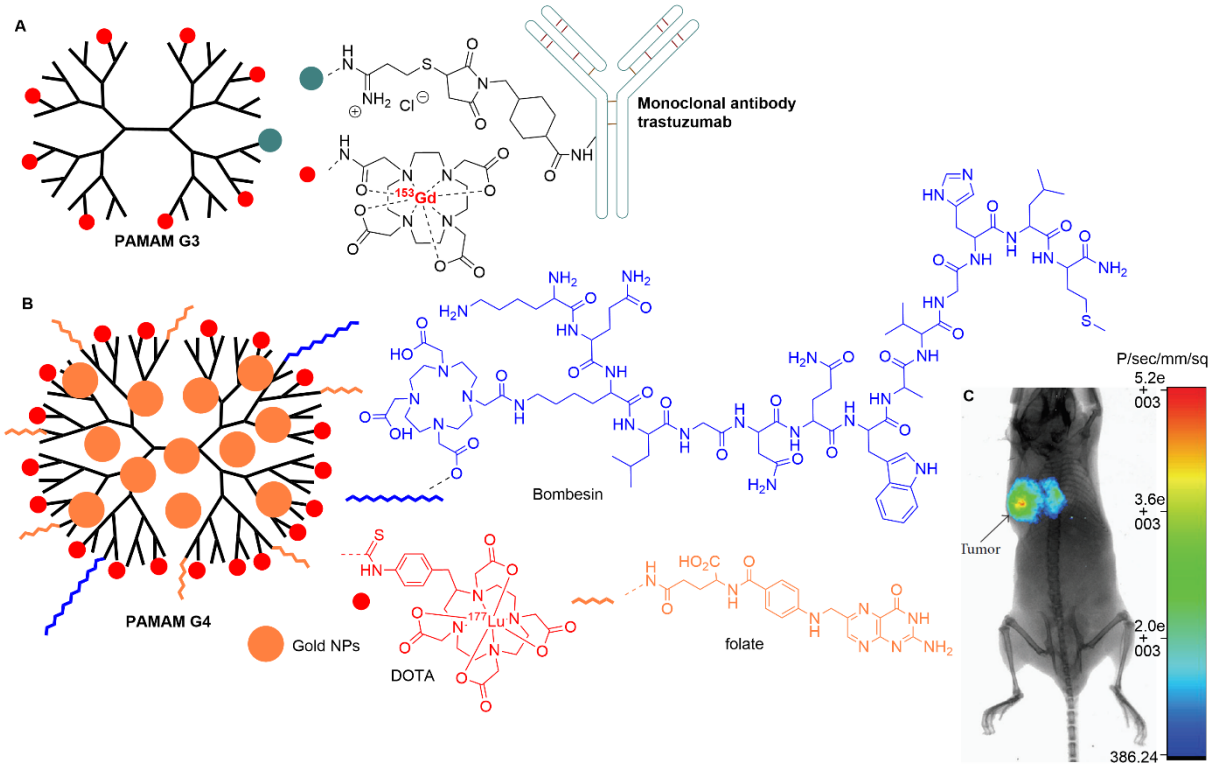

Figure 28. PAMAM dendrimers diversely functionalized, and used for the complexation of radionuclides. Part (C): Whole imaging of the body with an optical/X-ray imaging system using the ^{177}Lu DOTA complex shown in (B); image obtained 96 h after intratumoral administration (reproduced from ref. 113. Copyright the Authors, open access article).

5. Radioactive dendrimer complexes for PET imaging

Other types of dendritic radioactive complexes have been synthesized for positron emission tomography (PET) imaging. A review about dendrimers for PET imaging [88] and another about radioactive PAMAM dendrimers [89] have been published recently, thus only selected examples are given here. Two main radioactive elements have been complexed with dendrimers for PET imaging, gallium and copper. A generation 4 PAMAM dendrimer was functionalized with 48 DOTA ligands for the complexation of ^{68}Ga. PET images of mice after intravenous administration of this dendrimer revealed that 50% of the dendrimer was cleared from the blood circulation by 30 min. The dendrimer was excreted through the kidneys. For mice bearing tumors, a good non-specific uptake in tumor was observed, attributed to the EPR effect [114]. A triazacyclononane-triphosphinate (TRAP) chelator was used both as core and as branching unit in several dendritic molecules, functionalized on the surface with the prostate specific membrane antigen (PSMA) targeting the Glu-urea-Lys motif (Figure 29A). The macrocycles in these dendrimers were suitable for the complexation of ^{67}Ga (a γ-emitter for SPECT) and ^{68}Ga (a β^+-emitter for PET). Positron emission tomography (PET) images of a SCID mouse bearing a LNCaP (human prostate carcinoma) xenograft was obtained with the dendrimer complexing ^{68}Ga [115]. An amphiphilic dendron functionalized on the surface with the NOTA chelator, suitable for the complexation of ^{68}Ga for PET imaging was synthesized. It self-assembled in nanomicelles which were used to detect low-glucose-uptake in tumor-xenograft mouse models, thanks to the EPR effect (Figure 29B). Comparison with the clinical gold reference 2-fluorodeoxyglucose ([^{18}F]FDG) demonstrated that tumors of prostate cancer, glioblastoma cancers, colorectal cancer, and pancreatic cancer were more efficiently detected by the nanomicelles than by [^{18}F]FDG (Figure 29C) [116]. The same dendrons functionalized with the DOTA chelator, suitable for the complexation of ^{111}In for SPECT imaging were also synthesized (Figure 29B). Both compounds were used for imaging a mouse orthotopic xenograft model of pancreatic adenocarcinoma (SOJ-6) [117].

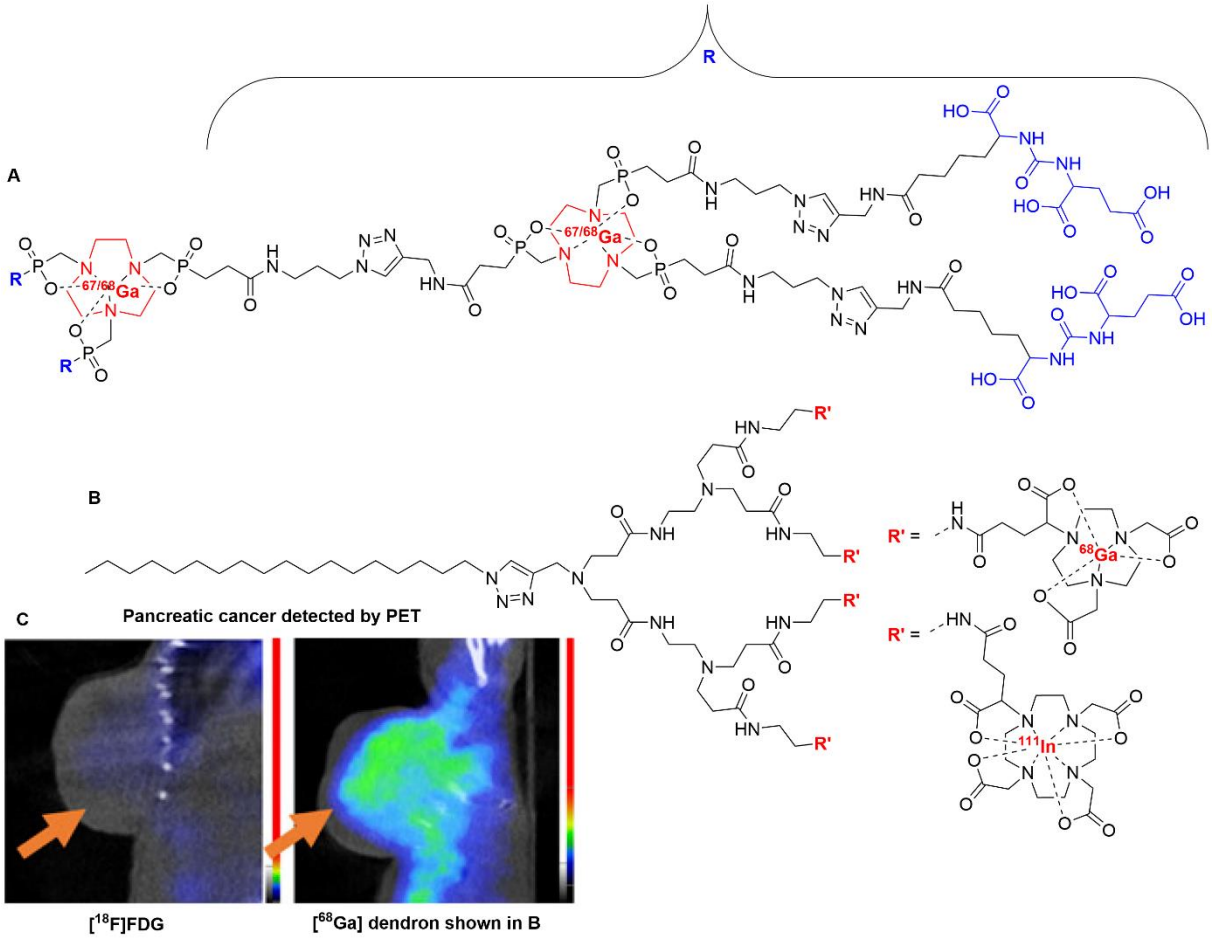

Figure 29. Dendrimers and dendrons for the complexation of radio-active ^{68}Ga and ^{111}In with, NOTA (A), DOTA or NOTA (B) ligands. Part (C): pancreatic cancer tumor detected by PET using the ^{68}Ga NOTA complex shown in (B) and comparison with [^{18}F]FGD (reproduced from ref. 116. Copyright the Authors, open access article).

Dendrimers radiolabeled with ^{64}Cu are the other family of dendrimer complexes suitable for PET imaging. A generation 4 PAMAM dendrimer bearing as terminal functions poly(L-lactide)-b-poly(ethylene glycol) conjugated with an anti-CD105 monoclonal antibody (TRC105) and NOTA, as a macrocyclic chelator for ^{64}Cu was synthesized for targeted imaging of cancer (Figure 30A). This compound was injected to 4T1 murine breast tumor-bearing mice, having a significant amount of CD105 expression during tumor growth. PET imaging demonstrated a high-level accumulation of this targeted dendrimer inside the tumor [118]. A PAMAM dendrimer ended by OH groups was used as support of poly(L-aspartate)-b-PEG copolymers, where the aspartate block was functionalized with a layer of conjugated doxorubicin (DOX). About 20% of the PEGs were functionalized at their end with the NODA (in fact NOTA) ligand for the chelation of Cu, and about 10% of the PEGs were functionalized with the F3 peptide (a 31-amino acid synthetic fragment), having a cell penetration capacity, especially in cancer cells (Figure 30B). This dendrimer loaded with ^{64}Cu complexed by the NOTA ligands was injected to mice bearing orthotopic MDA-MB-231 breast tumors. PET images demonstrated a high accumulation of this dendrimer in breast tumors [119]. A generation 5 PAMAM dendrimer was modified with folic acid (FA) and fluorescein isothiocyanate (FI), and radiolabeled with ^{64}Cu complexed by DOTA for dual imaging (PET and optical) of folate receptor (FR)-expressing tumors (Figure 30C). The tumor-targeting efficacy and biodistribution of the dendrimers were evaluated in nude mice bearing FR-positive KB tumor xenografts. Deceptively, a relatively high accumulation and retention of the dendrimers in mouse liver was observed, which might be due to the demetallation of the DOTA complex, pointing the necessity to find better chelation systems for Cu [120]. A very small PAMAM

dendrimer (generation 0) was also functionalized for dual mode imaging PET/optical. Three of the four functions were equipped with the NIRF dye Cy5.5, a DOTA metal chelator, and anti-HER2 Affibody for binding with the transmembrane protein HER2, a well-established tumor biomarker (Figure 30D). The ^{64}Cu-loaded dendrimer was used for dual-modality imaging (NIRF and PET) of SKOV3 tumor-bearing mice. A high tumor uptake, good tumor contrast, and high specificity were observed with this small dendrimer, along with favorable pharmacokinetic properties [121]. A small dendron based on lysine and cysteine was specifically elaborated for the detection of macrophages accumulation for the diagnostic and prognostic of atherosclerotic plaques. Four cyclic 9-aminoacid peptides LyP-1 (CGNKRTRGC), suitable for the binding to p32 proteins on activated macrophages was linked to the surface of the dendron, whereas the core comprised a 6-BAT ligand (6-[p-(bromoacetamido)benzyl]-1,4,8,11-tetraazacyclotetradecane-1,4,8,11-tetraacetic acid) suitable for the complexation of ^{64}Cu. Another dendron functionalized with 4 linear peptides of type ARAL was also synthesized, in the solid phase in both cases (Figure 30E). These dendrons were injected to atherosclerotic (ApoE−/−) mice. PET-CT co-registered images demonstrated greater uptake of the $(LyP\text{-}1)_4$-dendron-^{64}Cu than the $(ARAL)_4$-dendron-^{64}Cu in the aortic root and descending aorta of mice, confirming the efficiency of the targeting strategy (Figure 30F). [122]

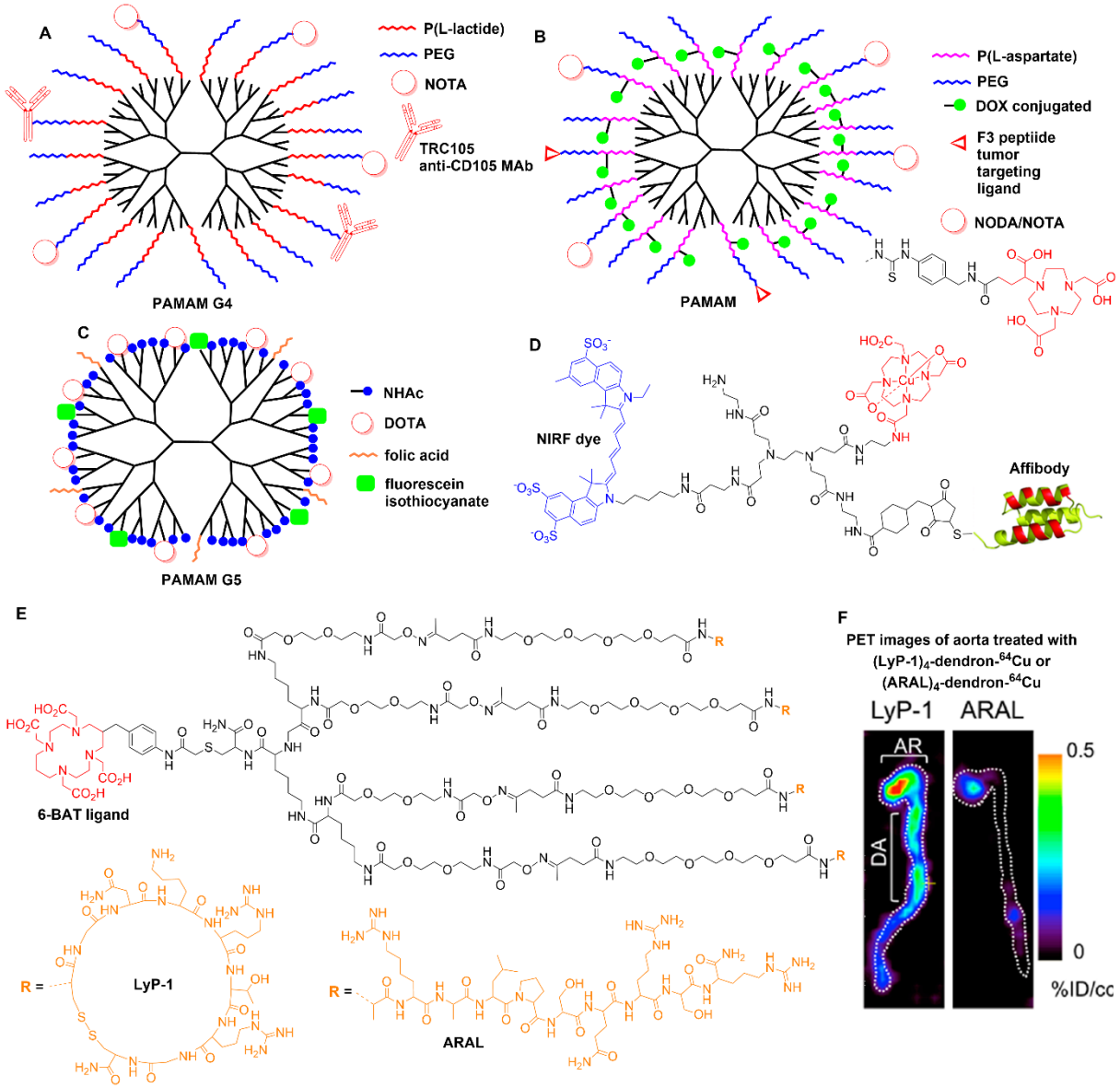

Figure 30. Dendrimers and dendrons for the complexation of radio-active ^{64}Cu. Part (F) PET images of atherosclerotic plaques in mice aorta treated with the ^{64}Cu complex of the dendrons shown in (E) (reproduced from ref. 122. Copyright K.W. Ferrara et al., open access article).

6. Conclusion

This review focused on the recent results concerning dendrimer metal complexes and their use for diverse types of imaging techniques (OI, MRI, SPECT, and PET), essentially *in vivo*. Optical imaging with dendrimers in which the optical properties are due to a metal complex are very rare. In fact, optical imaging with dendrimers is almost exclusively due to the grafting of organic fluorophores to dendrimers, either on their surface, to their core, or even in their branches [20]. These organic fluorophores are commercially available with suitable functions for grafting, are able to afford bright fluorescence in water after one-photon, or eventually two-photon absorption, thus there is no urgent necessity to have dendrimers functionalized with fluorescent metal complexes.

In contrast to optical imaging, magnetic resonance imaging with dendrimer metal complexes has been, and is currently widely studied. It constitutes the most important use of dendrimer complexes in bioimaging. The main advantage that is generally observed with dendrimers is a significant contrast enhancement in the MR images compared to the commercial contrast agents clinically used. This enhancement is due to the presence of a large number of paramagnetic agents in a single entity. The second advantage is the increased time during which the MR imaging can be performed. Extravasation of (small) commercial contrast agents in mice occurs after a few minutes, whereas MR imaging with dendrimer complexes can be performed for several hours, and in some cases several days after injection, with still a good contrast. The large size of dendrimers allows longer circulation times and prevents their rapid extravasation, but opens the question of their mode of elimination from the body. To avoid this problem, several biodegradable dendrimers, generally based on polyester branches, have been proposed. The large number of functions on the surface of dendrimers enables the stochastic grafting of several types of functions, for instance contrast agents together with fluorescent entities, and functions suitable for targeting cancerous cells. Such multifunctional dendrimers are usable for dual imaging by MRI and OI. However, albeit convenient for research, such approach affords ill-defined compounds that will be difficult to bring to clinical trials. Another property of dendrimers is the presence of internal voids, that could accommodate nanoparticles. This property has been used in particular for entrapping gold nanoparticles in dendrimers functionalized on their surface with MRI contrast agents, enabling dual imaging by MRI thanks to the dendrimer, and by CT thanks to the gold NPs. Multi imaging MRI/CT/OI has been even proposed with dendrimers functionalized on the surface with both contrast agents and fluorescent entities, and entrapping gold NPs in their internal voids. However, in this case also, the stochastic grafting of functions is certainly more suitable for research than for practical clinical uses. A large majority of studies concerning dendrimers for MRI are based on gadolinium complexes, due to the known efficiency of gadolinium ions as contrast agents. However, to overcome the known toxicity of gadolinium(III) ions in particular towards the kidney function [123], other metals have been proposed. Manganese(II) is less toxic than other paramagnetic ions, but has a lower relaxivity, which could be overcome by conjugating multiple Mn complexes on the surface of dendrimers. This is another advantage afforded by dendrimers as supports of MRI agents, which should be developed.

The complexation of radionuclides by dendrimers is also widely studied. Two main types of imaging techniques have been applied, depending on the type of radio-active elements, more precisely on the type of emission of the radioisotope, and on the energy range it emits. Single Photon Emission Computed Tomography (SPECT) imaging using dendrimer complexes has been essentially carried with the metastable isotope of technetium, ^{99m}Tc, even if ^{111}In, which is a γ-emitter as ^{99m}Tc, has also been used several times for SPECT imaging. This technique was applied to dendrimers for two different purposes: i) the detection of the biodistribution in the different organs, together with the rate of excretion of the dendrimers from the mice body, and ii) the detection of tumors and metastases in mice. The presence of multiple functions on the surface of dendrimers enables dual imaging combining different techniques. Such association offers a great advantage for image processing and quantification.

PET imaging is generally carried out with lighter elements than those used in SPECT, as it is based on the secondary emission of γ-photons by these elements emitting positrons. PET studies with dendritic

complexes of radioactive elements are essentially based on two radionuclides: ^{64}Cu and ^{68}Ga. These complexes have been used essentially for the detection of aggregations, generally of tumors, but also of atherosclerotic plaques. The non-specific targeting of tumors by radioactive dendrimers or dendrons has been observed in several cases, and attributed to the EPR effect. This is a major difference between dendrimers/dendrons and monomeric analogues, which has been illustrated by comparison with the clinical gold reference 2-fluorodeoxyglucose ([^{18}F]FDG). Of course, specific targeting generally increases the selectivity of the tumor detection, but the influence is majored by the EPR effect.

Despite a large number of publications, and extensive studies on animals, clinical trials with such dendritic complexes are very rare. To the best of our knowledge, only two small clinical studies have been performed a long time ago with gadolinium complexes, but have not been prolonged [124]. Both trials used a polylysine dendrimer, functionalized with 24 macrocyclic complexes of gadolinium on the surface, and named Gadomer-17 or SH L 643 A (Schering AG, Berlin, Germany). It was injected first in a Phase 1 clinical trial to 8 male healthy volunteers for imaging their aortoiliac region. No serious adverse events and no significant changes in laboratory parameters and vital signs occurred [125]. In a second clinical trial, the same dendrimer was injected to twelve patients (seven men, five women; age range, 46-78 years; mean age, 61.3 years) with angiographically proved coronary artery disease. This dendrimer improved detection of coronary artery disease at three-dimensional MR coronary angiography [126]. Noteworthy, another clinical trial is ongoing with a dendrimer complexing radioactive ^{188}Re, for both imaging and treatment in patients with inoperable liver cancer non-responding to conventional therapy [127]. Indeed, another use of dendrimer complexes in biology concerns fighting against cancers. Many publications concern this field, but there are very few clinical trials in this topic as well [128], and the use of dendrimers against cancers is outside of the present review.

Taken together, it is clear that dendrimer complexes offer many opportunities in biology, but despite a number of exciting results, there is very poor translation to practical uses. This is “the dendrimer paradox - high medical expectations but poor clinical translation” [129]. Such translation becomes an urgent necessity to continue to develop the field of dendrimers in biology, but it still constitutes a very difficult challenge.

7. References

[1] M.L. Etheridge, S.A. Campbell, A.G. Erdman, C.L. Haynes, S.M. Wolf, J. McCullough, Nanomedicine: NBM, 9 (2013) 1-14.
[2] F. Caruso, T. Hyeon, V.M. Rotello, Chem. Soc. Rev., 41 (2012) 2537-2538.
[3] T.L. Doane, C. Burda, Chem. Soc. Rev., 41 (2012) 2885-2911.
[4] G. Chen, I. Roy, C. Yang, P.N. Prasad, Chem. Rev., 116 (2016) 2826-2885.
[5] A. Wicki, D. Witzigmann, V. Balasubramanian, J. Huwyler, J. Control. Release, 200 (2015) 138-157.
[6] N. Lewinski, V. Colvin, R. Drezek, Small, 4 (2008) 26-49.
[7] S. Sharifi, S. Behzadi, S. Laurent, M.L. Forrest, P. Stroeve, M. Mahmoudi, Chem. Soc. Rev., 41 (2012) 2323-2343.
[8] A. Elsaesser, C.V. Howard, Adv. Drug Deliv. Rev., 64 (2012) 129-137.
[9] A.M. Caminade, C.O. Turrin, R. Laurent, A. Ouali, B. Delavaux-Nicot, Eds, Dendrimers: Towards Catalytic, Material and Biomedical Uses, John Wiley & Sons Ltd., Chichester, UK, 2011.
[10] D.A. Tomalia, H. Baker, J. Dewald, M. Hall, G. Kallos, S. Martin, J. Roeck, J. Ryder, P. Smith, Polymer J., 17 (1985) 117-132.
[11] E. Buhleier, F. Wehner, F. Vögtle, Synthesis, 78 (1978) 155-158.
[12] E.M.M. de Brabander van den Berg, E.W. Meijer, Angew. Chem.-Int. Edit. Engl., 32 (1993) 1308-1311.
[13] A.M. Caminade, S. Fruchon, C.O. Turrin, M. Poupot, A. Ouali, A. Maraval, M. Garzoni, M. Maly, V. Furer, V. Kovalenko, J.P. Majoral, G.M. Pavan, R. Poupot, Nat. Commun., 6 (2015) 7722.
[14] D.A. Tomalia, L.A. Reyna, S. Svenson, Biochem. Soc. Trans., 35 (2007) 61-67.
[15] M. Shen, Y. Huang, L. Han, J. Qin, X. Fang, J. Wang, V.C. Yang, J. Control. Release, 161 (2012) 884-892.
[16] M.A. Pysz, S.S. Gambhir, J.K. Willmann, Clin. Radiol. 65 (2010) 500-516.
[17] P. Govender, B. Therrien, G.S. Smith, Eur. J. Inorg. Chem., (2012) 2853-2862.
[18] S. Kunjachan, J. Ehling, G. Storm, F. Kiessling, T. Lammers, Chem. Rev., 115 (2015) 10907-10937.

[19] J.E. Talmadge, R.K. Singh, I.J. Fidler, A. Raz, Amer. J. Pathol. 170 (2007) 793-804.
[20] A.M. Caminade, A. Hameau, J.P. Majoral, Chem.-Eur. J., 15 (2009) 9270-9285.
[21] M.A. Alcala, C.M. Shade, H. Uh, S.Y. Kwan, M. Bischof, Z.P. Thompson, K.A. Gogick, A.R. Meier, T.G. Strein, D.L. Bartlett, R.A. Modzelewski, Y.J. Lee, S. Petoud, C.K. Brown, Biomaterials, 32 (2011) 9343-9352.
[22] M.A. Alcala, S.Y. Kwan, C.M. Shade, M.G. Lang, H. Uh, M.Y. Wang, S.G. Weber, D.L. Bartlett, S. Petoud, Y.J. Lee, Nanomedicine: NBM, 7 (2011) 249-258.
[23] C.M. Andolina, P.J. Klemm, W.C. Floyd, J.M.J. Frechet, K.N. Raymond, Macromolecules, 45 (2012) 8982-8990.
[24] K.Y. Zhang, H.W. Liu, T.T.H. Fong, X.G. Chen, K.K.W. Lo, Inorg. Chem., 49 (2010) 5432-5443.
[25] A. Ruggi, C. Beekman, D. Wasserberg, V. Subramaniam, D.N. Reinhoudt, F.W.B. van Leeuwen, A.H. Velders, Chem.-Eur. J., 17 (2011) 464-467.
[26] K. Qiu, B. Yu, H. Huang, P. Zhang, J. Huang, S. Zou, Y. Chen, L. Ji, H. Chao, Sci. Rep., 5 (2015) 10707.
[27] S.M. Vithanarachchi, M.J. Allen, Curr. Mol. Imaging, 1 (2012) 12-25.
[28] G.P. Yan, L. Robinson, P. Hogg, Radiography, 13 (2007) e5-e19.
[29] E.C. Wiener, M.W. Brechbiel, H. Brothers, R.L. Magin, O.A. Gansow, D.A. Tomalia, P.C. Lauterbur, Mag. Reson. Med., 31 (1994) 1-8.
[30] E. Toth, D. Pubanz, S. Vauthey, L. Helm, A.E. Merbach, Chem.-Eur. J., 2 (1996) 1607-1615.
[31] J.M. Bryson, J.W. Reineke, T.M. Reineke, Macromolecules, 45 (2012) 8939-8952.
[32] Z. Qiao, X. Shi, Prog. Polym. Sci., 44 (2015) 1-27.
[33] L. Ding, Z. Lyu, D. Dhumal, C.L. Kao, M. Bernard, L. Peng, Sci. China Mater., 61 (2018) 1420-1443.
[34] N. Kosaka, M. Bernardo, M. Mitsunaga, P.L. Choyke, H. Kobayashi, Contrast Media Mol. Imaging, 7 (2012) 247-253.
[35] K. Sano, T. Temma, T. Azuma, R. Nakai, M. Narazaki, Y. Kuge, H. Saji, Mol. Imaging Biol., 13 (2011) 1196-1203.
[36] L. Han, J. Li, S. Huang, R. Huang, S. Liu, X. Hu, P. Yi, D. Shan, X. Wang, H. Lei, C. Jiang, Biomaterials, 32 (2011) 2989-2998.
[37] R. Mustafa, B. Zhou, J. Yang, L. Zheng, G. Zhang, X. Shi, RSC Adv., 6 (2016) 95112.
[38] T. Tang, X. Ma, Y. Bian, Z. Yuan, D. Zou, N. Chen, ACS Biomater. Sci. Eng., 5 (2019) 1978-1986.
[39] L. Guo, H. Shi, H. Wu, Y. Zhang, X. Wang, D. Wu, L. An, S. Yang, Carbon, 107 (2016) 87-99.
[40] K. Nwe, D. Milenic, L.H. Bryant, C.A.S. Regino, M.W. Brechbiel, J. Inorg. Biochem., 105 (2011) 722-727.
[41] C.H. Huang, K. Nwe, A. Al Zaki, M.W. Brechbiel, A. Tsourkas, ACS Nano, 6 (2012) 9416-9424.
[42] K. Karki, J.R. Ewing, M.M. Ali, J. Nanomed. Nanotechnol., 7 (2016) 4. DOI: 10.4172/2157-7439.1000395
[43] L. Zhang, N.R. Varma, Z.Z. Gang, J.R. Ewing, A.S. Arbab, M.M. Ali, J. Nanomed. Nanotechnol., 7 (2016) 5. DOI: 10.4172/2157-7439.1000404
[44] H. Yan, J. Wang, P. Yi, H. Lei, C. Zhan, C. Xie, L. Feng, J. Qian, J. Zhu, W. Lu, C. Li, Chem. Commun., 47 (2011) 8130-8132.
[45] H. Yan, L. Wang, J. Wang, X. Weng, H. Lei, X. Wang, L. Jiang, J. Zhu, W. Lu, X. Wei, C. Li, ACS Nano, 6 (2012) 410-420.
[46] Y. Cao, G. Zu, Y. Kuang, Y. He, Z. Mao, M. Liu, D. Xiong, R. Pei, ACS Appl. Mater. Interfaces, 10 (2018) 26906-26916.
[47] S. Gunduz, N. Nitta, S. Vibhute, S. Shibata, M.E. Mayer, N.K. Logothetis, I. Aoki, G. Angelovski, Chem. Commun., 51 (2015) 2782-2785.
[48] F. Garello, S. Gunduz, S. Vibhute, G. Angelowski, E. Terreno, J. Mater. Chem. B, 8 (2020) 969-979.
[49] L. Connah, G. Angelovski, Biomacromolecules, 19 (2018) 4668-4676.
[50] S. Wen, K. Li, H. Cai, Q. Chen, M. Shen, Y. Huang, C. Peng, W. Hou, M. Zhu, G. Zhang, X. Shi, Biomaterials, 34 (2013) 1570-1580.
[51] K. Li, S. Wen, A.C. Larson, M. Shen, Z. Zhang, Q. Chen, X. Shi, G. Zhang, Int. J. Nanomed., 8 (2013) 2589-2600.
[52] Y. Fan, W. Tu, M. Shen, X. Chen, Y. Ning, J. Li, T. Chen, H. Wang, F. Yin, Y. Liu, X. Shi, Adv. Funct. Mater., 30 (2020) 1909285.
[53] Q. Chen, K. Li, S. Wen, H. Liu, C. Peng, H. Cai, M. Shen, G. Zhang, X. Shi, Biomaterials, 34 (2013) 5200-5209.
[54] Q. Chen, H. Wang, H. Liu, S. Wen, C. Peng, M. Shen, G. Zhang, X. Shi, Anal. Chem., 87 (2015) 3949-3956.
[55] J. Liu, Z. Xiong, J. Zhang, C. Peng, B. Klajnert-Maculewicz, M. Shen, X. Shi, ACS Appl. Mater. Interfaces, 11 (2019) 15212-15221.
[56] J. Chen, Y. sun, Q. Chen, L. Wang, S. Wang, Y. Tang, X. Shi, H. Wang, Nanoscale, 8 (2016) 13568.
[57] K. Luo, G. Liu, B. He, Y. Wu, Q. Gong, B. Song, H. Ai, Z. Gu, Biomaterials, 32 (2011) 2575-2585.

[58] K. Luo, G. Liu, W. She, Q. Wang, G. Wang, B. He, H. Ai, Q. Gong, B. Song, Z. Gu, Biomaterials, 32 (2011) 7951-7960.
[59] H. Li, P. Wang, W. Gong, Q. Wang, J. Zhou, W.-H. Zhu, Y. Cheng, Adv. Healthcare Mater., 7 (2018) 1700912.
[60] J. Li, S. Huang, K. Shao, Y. Liu, S. An, Y. Kuang, Y. Guo, H. Ma, X. Wang, C. Jiang, Sci. Rep., 3 (2013) 1623. DOI: 10.1038/srep01623
[61] J. Lim, B. Turkbey, M. Bernardo, L.H. Bryant, M. Garzoni, G.M. Pavan, T. Nakajima, P.L. Choyke, E.E. Simanek, H. Kobayashi, Bioconjugate Chem., 23 (2012) 2291-2299.
[62] M. Ye, Y. Qian, Y. Shen, H. Hu, M. Sui, J. Tang, J. Mater. Chem., 22 (2012) 14369-14377.
[63] T. Li, Y. Qian, M. Ye, J. Tang, H. Hu, Y. Shen, Chin. J. Chem., 32 (2014) 91-96.
[64] M. Ye, Y. Qian, J. Tang, H. Hu, M. Sui, Y. Shen, J. Control. Release, 169 (2013) 239-245.
[65] Y. Han, X. Zhou, Y. Qian, H. Hu, Z. Zhou, X. Liu, J. Tang, Y. Shen, Biomaterials, 213 (2019) 119195. DOI: 10.1016/j.biomaterials.2019.05.006
[66] W.T. Chen, T.T.F. Shih, R.C. Chen, S.Y. Tu, H. Wen-Yuen, P.C. Yang, Mol. Imaging, 11 (2012) 286-300.
[67] M. Mirzaei, M. Mohagheghi, D. Shahbazi-Gahrouei, A. Khatami, J. Nanomed. Nanothechnol., 3 (2012) 7, 1000147. DOI:10.4172/2157-7439.1000147
[68] N. Ghalandarlaki, T.D. Mohammadi, R. Agha Babaei, M.A. Tabasi, P. Keyhanvar, B. Mehravi, P. Yaghmaei, R.A. Cohan, M.S. Ardestani, Drug Research 64 (2014) 57-65.
[69] N. Hashempour Alamdari, M. Alaei-Beirami, S.A. Sadat Shandiz, H. Hejazinia, R. Rasouli, M. Saffari, S.E. Sadat Ebrahimi, A. Assadi, M. Shafiee Ardestani, Contrast Media Mol. Imaging, 2017 (2017) 3625729-3625729.
[70] I. Jacobs, G.J. Strijkers, H.M. Keizer, H.M. Janssen, K. Nicolay, M.C. Schabel, Magnetic Res. Med., 75 (2016) 1142-1153.
[71] Z. Xiong, Y. Wang, J. Zhu, Y. He, J. Qu, C. Effenberg, J.Xia, D. Appelhans, X. Shi, Biomater. Sci., 4 (2016) 1622-1629.
[72] Y. Han, Y. Qian, X. Zhou, H. Hu, X. Liu, Z. Zhou, J. Tang, Y. Shen, Polym. Chem. 7 (2016) 6354-6362.
[73] Y. Miyake, Y. Kimura, S. Ishikawa, H. Tsujita, H. Miura, M. Narazaki, T. Matsuda, Y. Tabata, T. Yano, A. Toshimitsu, T. Kondo, Tetrahedron Lett., 53 (2012) 4580-4583.
[74] Y. Miyake, S. Ishikawa, Y. Kimura, A. Son, H. Imai, T. Matsuda, H. Yamada, A. Toshimitsu, T. Kondo, Sensors, 15 (2015) 31973–31986.
[75] L. Granato, D. Longo, S. Boutry, L. Vander Elst, C. Henoumont, S. Aime, R.N. Muller, S. Laurent, Chem. Biodiversity, 16 (2019) e1900322.
[76] Z. Zhou, M. Qutaish, Z. Han, R.M. Schur, Y.Liu, D.L. Wilson, Z.R. Lu, Nat. Commun. 6 (2015) 7984.
[77] F. Fernandez-Trillo, J. Pacheco-Torres, J. Correa, P. Ballesteros, P. Lopez-Larrubia, S. Cerdan, R. Riguera, E. Fernandez-Megia, Biomacromolecules, 12 (2011) 2902-2907.
[78] Y. Li, T.Y. Lin, Y. Luo, Q. Liu, W. Xiao, W. Guo, D. Lac, H. Zhang, C. Feng, S. Wachsmann-Hogiu, J.H. Walton, S.R. Cherry, D.J. Rowland, D. Kukis, C. Pan, K.S. Lam, Nat. Commun. 5 (2014) 4712.
[79] C. Guo, L. Sun, W. She, N. Li, L. Jiang, K. Luo, Q. Gong, Z. Gu, Polymer Chem., 7 (2016) 2531-2541.
[80] C. Guo, L. Sun, H. Cai, Z. Duan, S. Zhang, Q. Gong, K. Luo, Z. Gu, Acs Appl. Mater. Interfaces, 9 (2017) 23508-23519.
[81] M. Tan, Z. Ye, E.K. Jeong, X. Wu, D.L. Parker, Z.R. Lu, Bioconjugate Chem., 22 (2011) 931-937.
[82] R. Wang, Y. Luo, S. Yang, J. Lin, D. Gao, Y. Zhao, J. Liu, X. Shi, X. Wang, Sci. Rep., 6 (2016) 33844.
[83] P.M Winter, WIREs Nanomed. Nanobiotechnol. 4 (2012) 389-398.
[84] M.M. Ali, M.P.I. Bhuiyan, B. Janic, N.R.S. Varma, T. Mikkelsen, J.R. Ewing, R.A. Knight, M.D. Pagel, A.S. Arbab, Nanomedicine, 7 (2012) 1827-1837.
[85] S. Gonawala, M.M. Ali, J. Nanomed. Nanotechnol., 8 (2017) DOI:10.4172/2157-7439.1000444
[86] C. Ghobril, G. Lamanna, M. Kueny-Stotz, A. Garofalo, C. Billotey, D. Felder-Flesch, New J. Chem., 36 (2012) 310-323.
[87] L. Zhao, M. Zhu, Y. Li, Y. Xing, J. Zhao, Molecules (Basel, Switzerland), 22 (2017) 1350.
[88] L. Zhao, X. Shi, J. Zhao, Drug Deliv., 24 (2017) 81-93.
[89] T. Xiao, D. Li, X. Shi, M. Shen, Macromol. Biosci. 20 (2020) 1900282
[90] T. Kniess, M. Laube, F. Wüst, J. Pietzsch, Dalton Trans., 46 (2017) 14435-14451.
[91] M.R. Tassano, P.F. Audicio, J.P. Gambini, M. Fernandez, J.P. Damian, M. Moreno, J.A. Chabalgoity, O. Alonso, J.C. Benech, P. Cabral, Bioorg. Med. Chem. Lett., 21 (2011) 5598-5601.
[92] X. Xu, Y. Zhang, X. Wang, X. Guo, X. Zhang, Y. Qi, Y.M. Shen, Bioorg. Med. Chem., 19 (2011) 1643-1648.
[93] J.M. Criscione, L.W. Dobrucki, Z.W. Zhuang, X. Papademetris, M. Simons, A.J. Sinusas, T.M. Fahmy, Bioconjugate Chem., 22 (2011) 1784-1792.
[94] X. Li, Z. Xiong, X. Xu, Y. Luo, C. Peng, M. Shen, X. Shi, ACS Appl. Mater. Interfaces, 8 (2016) 19883-19891.

[95] Y. Li, L. Zhao, X. Xu, N. Sun, W. Qiao, Y. Xing, M. Shen, M. Zhu, X. Shi, J. Zhao, J. Biomed. Nanotechnol., 15 (2019) 1201-1212.
[96] X. Xu, L. Zhao, X. Li, P. Wang, J. Zhao, X. Shi, M. Shen, Biomater. Sci., 5 (2017) 2393-2397.
[97] S. Wen, L. Zhao, Q. Zhao, D. Li, C. Liu, Z. Yu, M. Shen, J.-P. Majoral, S. Mignani, J. Zhao, X. Shi, J. Mater. Chem. B, 5 (2017) 3810-3815.
[98] Y. Luo, L. Zhao, X. Li, J. Yang, L. Guo, G. Zhang, M. Shen, J. Zhao, X. Shi, J. Mater. Chem. B, 4 (2016) 7220-7225.
[99] A. Narmani, K. Yavari, J. Mohammadnejad, Colloids Surf. B, 159 (2017) 232-240.
[100] M. Song, Z. Guo, M. Gao, C. Shi, D. Xu, L. You, X. Wu, X. Su, R. Zhuang, W. Pan, T. Liu, X. Zhang, Chem. Biol. Drug Des., 89 (2017) 755-761.
[101] S.A. McNelles, S.D. Knight, N. Janzen, J.F. Valliant, A. Adronov, Biomacromolecules, 16 (2015) 3033-3041.
[102] A.G. Khosroshahi, M. Amanlou, O. Sabzevari, F.J. Daha, M.R. Aghasadeghi, M. Ghorbani, M.S. Ardestani, M.S. Alavidjeh, S.M. Sadat, M.H. Pouriayevali, L. Mousavi, S.E.S. Ebrahimi, Curr. Med. Chem., 20 (2013) 123-133.
[103] M.S. Ardestani, A. Bitarafan-Rajabi, P. Mohammadzadeh, S. Mortazavi-Derazkola, O. Sabzevari, A.D. Azar, S. Kazemi, S.R. Hosseini, S.M. Ghoreishi, Bioorg. Chem. 96 (2020) 103572.
[104] N. Mohtavinejad, M. Amanlou, A. Bitarafan-Rajabi, A. Khalaj, A. Pormohammad, M.S. Ardestani, Bioorg. Chem. 98 (2020) 103731.
[105] V. Biricova, A. Laznickova, M. Laznicek, M. Polasek, P. Hermann, J. Pharm. Biomed. Anal., 56 (2011) 505-512.
[106] C. Kojima, Y. Niki, M. Ogawa, Y. Magata, Int. J. Pharm., 476 (2014) 164-168.
107] K. Sano, Y. Iwamiya, T. Kurosaki, M. Ogawa, Y. Magata, H. Sasaki, T. Ohshima, M. Maeda, T. Mukai, J. Control. Release, 194 (2014) 310-315.
[108] S. Matsuura, H. Katsumi, H. Suzuki, N. Hirai, H. Hayashi, K. Koshino, T. Higuchi, Y. Yagi, H. Kimura, T. Sakane, A. Yamamoto, Proc. Natl. Acad. Sci. U. S. A., 115 (2018) 10511-10516.
[109] S. Matsuura, H. Katsumi, H. Suzuki, N. Hirai, R. Takashima, M. Morishita, T. Sakane, A. Yamamoto, Pharmaceutics, 10 (2018) 251.
[110] H. Katsumi, R. Takashima, H. Suzuki, N. Hirai, S. Matsuura, H. Kimuira, M. Morishita, A. Yamamoto, Free Radical Res. (2019) DOI:10.1080:10715762.2019.1697437.
[111] J. Kuil, T. Buckle, J. Oldenburg, H.S. Yuan, A.D. Borowsky, L. Josephson, F.W.B. van Leeuwen, Mol. Pharm., 8 (2011) 2444-2453.
[112] H. Rahmania, A. Mutalib, M. Ramli, J. Levita, J. Rad. Res. Appl. Sci., 8 (2015) 91-99.
[113] H. Mendoza-Nava, G. Ferro-Flores, F.M. Ramírez, B. Ocampo-García, C. Santos-Cuevas, L. Aranda-Lara, E. Azorín-Vega, E. Morales-Avila, K. Isaac-Olivé, J. Nanomater. (2016) 1039258. DOI:10.1155/2016/1039258
[114] A. Ghai, B. Singh, P.P. Hazari, M.K. Schultz, A. Parmar, P. Kumar, S. Sharma, D. Dhawan, A.K. Mishra, Appl. Radiat. Isot., 105 (2015) 40-46.
[115] D. Reich, A. Wurzer, M. Wirtz, V. Stiegler, P. Spatz, J. Pollmann, H.-J. Wester, J. Notni, Chem. Commun., 53 (2017) 2586-2589.
[116] P. Garrigue, J. Tang, L. Ding, A. Bouhlel, A. Tintaru, E. Laurini, Y. Huang, Z. Lyu, M. Zhang, S. Fernandez, L. Balasse, W. Lan, E. Mas, D. Marson, Y. Wen, X. Liu, S. Giorgi, J. Iovanna, S. Pricl, B. Guillet, L. Peng, Proc. Natl. Acad. Sci. U. S. A., 115 (2018) 11454-11459.
[117] L. Ding, Z. Lyu, A. Tintaru, E. Laurini, D. Marson, B. Louis, A. Bouhlet, L. Balasse, S. Fernandez, P. Garrigue, E. Mas, S. Giogio, S. Pricl, B. Guillet, L. Peng, Chem. Comm., 56 (2020) 301-304.
[118] J. Guo, H. Hong, G. Chen, S. Shi, Q. Zheng, Y. Zhang, C.P. Theuer, T.E. Barnhart, W. Cai, S. Gong, Biomaterials, 34 (2013) 8323-8332.
[119] J. Yang, W. Lu, J. Xiao, Q. Zong, H. Xu, Y. Yin, H. Hong, W. Xu, Acta Biomater., 79 (2018) 306-316.
[120] W. Ma, F. Fu, J. Zhu, R. Huang, Y. Zhu, Z. Liu, J. Wang, P.S. Conti, X. Shi, K. Chen, Nanoscale, 10 (2018) 6113-6124.
[121] Y. Wang, Z. Miao, G. Ren, Y. Xu, Z. Cheng, Chem. Comm. 50 (2014) 12832-12835
[122] J.W. Seo, H. Baek, L.M. Mahakian, J. Kusunose, J. Hamzah, E. Ruoslahti, K.W. Ferrara, Bioconjugate Chem., 25 (2014) 231-239.
[123] M. Sieber, P. Lengsfeld, J. Walter, H. Schirmer, T. Frenzel, F. Siegmund, H. Weinmann, H. Pietsch, J. Magn. Reson. Imaging 27 (2008) 955-962.
[124] V.M. Runge, J.T. Heverhagen, Invest. Radiol., 53 (2018) 381-389.
[125] B. Tombach, J. Schneider, P. Reimer, M. Mahler, W. Ebert, K. Shamsi, W. Heindel, Proc. Intl. Soc. Mag. Reson. Med. 10 (2002)
[126] C.U. Herborn, M. Schmidt, O. Bruder, E. Nagel, K. Shamsi, J. Barkhausen, Radiology, 233 (2004) 567-573.

[127] https://clinicaltrials.gov/ct2/show/NCT03255343?term=dendrimer&draw=2&rank=5 (accessed October 14th, 2020)
[128] https://clinicaltrials.gov/ct2/results?cond=&term=dendrimer&cntry=&state=&city=&dist= (accessed October 14th, 2020)
[129] S. Svenson, Chem. Soc. Rev., 44 (2015) 4131-4144.